

# Temperature Control of Solar Air Conditioning Systems

By  
Carlos A. González Lozano

A thesis submitted in partial fulfillment of the requirements for the degree of

MASTER OF SCIENCE  
in  
ELECTRICAL ENGINEERING

UNIVERSITY OF PUERTO RICO  
MAYAGÜEZ CAMPUS  
2004

Approved by:

---

Jorge E. González Cruz, Ph.D.  
Member, Graduate Committee

---

Date

---

Miguel Vélez Reyes, Ph.D.  
Member, Graduate Committee

---

Date

---

Gerson Beauchamp Báez, Ph.D.  
President, Graduate Committee

---

Date

---

Frederick Just, Ph.D.  
Representative of Graduate Studies

---

Date

---

Jorge L. Ortiz Álvarez, Ph.D.  
Chairperson of the Department

---

Date

## Abstract

This thesis investigates the problem of regulating the temperature of a conditioned space using a Solar Assisted Air Conditioning Systems (SAACS) prototype located at Cabo Rojo, Puerto Rico. The SAACS Prototype consists of a 66 flat plate solar collector array with 115.4 m<sup>2</sup> of selective surface area, a 35 kW single-effect lithium-bromide absorption chiller, a 84 kW cooling tower, a 50 kW auxiliary hot water boiler, a 5700 liter storage tank equipped with flexible stratification manifolds, and a 1800 l/hr air-handling unit.

A discrete-time state-space model of the absorption chiller and a linear model of the plant to be controlled (the conditioned space) are identified and presented. Experimental data was used for the determination of these models.

A temperature controller was designed and applied to the plant model. This controller operates the absorption chiller under multiple load conditions and regulates the flow in the chilled water line based on the conditioned space requirements. The designed controller was implemented in the SAACS prototype. The system's performance under this temperature controller is analyzed and the results are presented and discussed.

## Resumen

Esta tesis considera el problema de regular la temperatura de un espacio acondicionado mediante un prototipo de sistema de acondicionador de aire asistido con energía solar (SAAS) localizado en Cabo Rojo, Puerto Rico. El sistema consiste de un arreglo de 66 colectores solares planos con una superficie selectiva de  $115.4 \text{ m}^2$ , una máquina de absorción de Bromuro de Litio con una capacidad de 35 kW, una torre de enfriamiento con capacidad de 84 kW, una caldera con capacidad de 50 kW como calentador de agua auxiliar, un tanque de almacenamiento de 5700 litros equipado con tubería de estratificación flexible y una manejadora de aire de 1800 litros por hora.

En esta tesis se desarrolla un modelo de tiempo discreto en variables de estado para la máquina de absorción y un modelo lineal de la planta a ser controlada (el espacio acondicionado). Se utilizaron datos experimentales para la determinación de estos modelos.

Un controlador de temperatura fue diseñado y aplicado al modelo de la planta. Este controlador permite operar la máquina de absorción bajo múltiples condiciones de carga y regula el flujo de la línea de agua fría basado en los requerimientos del espacio acondicionado. El controlador diseñado fue implementado al SAAS. El desempeño del sistema con el controlador de temperatura es analizado y se presentan y se discuten los resultados.

# Copyright

© Carlos Andres González Lozano, 2004  
ALL RIGHTS RESERVED

## **Dedication**

To my mother Maria Nancy and my Grandmother Bertha Lucia (God is with her), for their unconditional support, since no one have sacrificed more to see me achieve my goals. To my brothers, Luis Fernando, Diego Humberto, Alexis Mauricio and Julian David, whom I love so much. Finally to my nephew “Dieguito”, for making my life happier when I am in Colombia.

## Acknowledgments

This research was primarily sponsored by the National Science Foundation (NSF) under grant # DEAC36-83CH10093 through Universal Solar Products, A/C Mechanical Services and the University of Puerto Rico-Mayagüez Campus. Special thanks to all the members of the National Fish and Wildlife Service in Cabo Rojo, for their support and patience during this research and for providing us with the facilities to test the SAACS system.

The author would like to thank Dr. Gerson Beauchamp-Báez and Dr Jorge E. González for their unconditional support and guidance throughout this research. Thanks also go to all who cooperated in this research, especially to Eng. Héctor Sánchez III, Eng. Gerardo Cosme and Eng. Mario Colón.

Finally, special thanks to Dr. Miguel Vélez, Dr Frederick Just, Dr. Raúl Torres and Dr. José Fernando Vega who are excellent people and professors. Thank you for teaching me many things for my academic and personal life during my time at the Electrical and Computer Engineering Department.

# Table of Contents

List of Figures.....	ix
List of Tables.....	xii
Chapter 1.....	1
Introduction.....	1
1.1 Solar Air Conditioning Systems.....	1
1.2 Objective and Contributions.....	2
1.3 Thesis Outline.....	3
Chapter 2.....	4
Previous Work.....	4
2.1 Absorption Chiller Dynamic Modeling.....	4
2.2 System Modeling and Parameter Estimation of Absorption Machines.....	9
2.3 Temperature Control of HVAC Systems.....	11
2.4 Identification of Simple Process Models for Control Purposes.....	13
Chapter 3.....	15
SAACS Description and Data Acquisition System.....	15
3.1 SAACS Prototype Description.....	15
3.1.1 Absorption Machine and Air Handling Unit (AHU).....	17
3.1.2 Conditioned Space.....	19
3.2 Data Acquisition System.....	20
3.2.1 Hardware Configuration.....	20
3.2.2 Software Configuration.....	23
3.3 Experimental Approach.....	24
Chapter 4.....	26
System Modeling.....	26
4.1 System Identification and Parameter Estimation Theory.....	26
4.1.1 “Black Box” Discrete-Time Parameterizations.....	28
4.1.2 Discrete-Time Transfer Functions Parameterization.....	30
4.2 System Modeling Results.....	31
4.2.1 Absorption Machine Modeling.....	32

Residual Analysis for the Identification of the Absorption Machine Model.	39
Validation of the Absorption Machine Model.....	41
Residual Analysis for the Validation of the Absorption Machine Model.....	45
4.2.2 Conditioned Space Modeling.....	48
Chapter 5.....	55
Controller Design and Implementation.....	55
5.1 Temperature Controller Design.....	55
5.2 Temperature Controller Implementation.....	60
5.3 SAACS System’s Performance Analysis.....	67
Chapter 6.....	75
Conclusions and Recommendations.....	75
References.....	77

## List of Figures

<b>Figure 1:</b> Simple Block Diagram of Water-Bromide Single Effect Absorption Cycle.....	5
<b>Figure 2:</b> Schematic Diagram of the SAACS Prototype Located in Cabo Rojo, Puerto Rico.....	16
<b>Figure 3:</b> Absorption Chiller Control and Monitoring Schematics.....	18
<b>Figure 4:</b> Schematic Diagram of the Conditioned Space and its Sensors.....	19
<b>Figure 5:</b> GUI for the Data Acquisition.....	23
<b>Figure 6:</b> Schematic of the Experimental Setup.....	25
<b>Figure 7:</b> Experiment Data Set for System Identification of the Absorption Chiller (a) Inlet and Outlet Chilled Water Loop Temperature, (b) Inlet and Outlet Heat Medium Loop Temperature, and (c) Chilled Water Mass Flow Rate.....	34
<b>Figure 8:</b> Measured and Estimated Output for the 2 <sup>nd</sup> order state-space model (a) Inlet and Outlet Chilled Water Loop Temperature and (b) Inlet and Outlet Heat Medium Loop Temperature.....	36
<b>Figure 9:</b> Measured and Estimated Output for the 3 <sup>rd</sup> order state-space model (a) Inlet and Outlet Chilled Water Loop Temperature and (b) Inlet and Outlet Heat Medium Loop Temperature.....	37
<b>Figure 10:</b> Measured and Estimated Output for the 4 <sup>th</sup> order state-space model (a) Inlet and Outlet Chilled Water Loop Temperature and (b) Inlet and Outlet Heat Medium Loop Temperature.....	38
<b>Figure 11:</b> Residuals Errors for the 2 <sup>nd</sup> Order Discrete-Time State-Space Model (Left) and their Respective Autocorrelation .....	39
<b>Figure 12:</b> Residuals Errors for the 3 <sup>rd</sup> Order Discrete-Time State-Space Model (Left) and their Respective Autocorrelation .....	40
<b>Figure 13:</b> Residuals Errors for the 4 <sup>th</sup> Order Discrete-Time State-Space Model (Left) and their Respective Autocorrelation .....	40
<b>Figure 14:</b> Experimental Input Data for Validation of the Absorption Machine .....	41

<b>Figure 15:</b> Validation Test for the 2 <sup>nd</sup> Order Discrete-Time State-Space Model of the Absorption Machine .....	42
<b>Figure 16:</b> Validation Test for the 3 <sup>rd</sup> Order Discrete-Time State-Space Model of the Absorption Machine .....	43
<b>Figure 17:</b> Validation Test for the 4 <sup>th</sup> Order Discrete-Time State-Space Model of the Absorption Machine .....	44
<b>Figure 18:</b> Residual Errors of the Validation Test of the 2 <sup>nd</sup> Order Discrete-Time State-Space Model (Left) and their Respective Autocorrelation (Right) .....	45
<b>Figure 19:</b> Residual Errors of the Validation Test of the 3 <sup>rd</sup> Order Discrete-Time State-Space Model (Left) and their Respective Autocorrelation (Right) .....	46
<b>Figure 20:</b> Residual Errors of the Validation Test of the 4 <sup>th</sup> Order Discrete-Time State-Space Model (Left) and their Respective Autocorrelation (Right).....	46
<b>Figure 21:</b> Histograms of the Residual Errors (a) 2 <sup>nd</sup> Order Model, (b) 3 <sup>rd</sup> Order Model, and (c) 4 <sup>th</sup> Order Model .....	47
<b>Figure 22:</b> Experimental Data Set for Identification of the Conditioned Space (a) Conference Room temperature (b) Chilled Water Mass Flow Sequence .....	50
<b>Figure 23:</b> Measured and Estimated Output Given by the IDGREY Function .....	52
<b>Figure 24:</b> Validation Test for the Identification of the Temperature in the Conference Room.....	53
<b>Figure 25:</b> Residual Analysis for the Validation test (a) Residual Errors, (b) Autocorrelation of the Residual Errors, and (c) Histogram of the Residual Errors ....	54
<b>Figure 26:</b> Closed-Loop Control Structure for the Temperature Control in the Conditioned Space.....	56
<b>Figure 27:</b> Close Loop Step Response and PI Controller Response for the Conditioned Space Simulated with Matlab® .....	58
<b>Figure 28:</b> Simulink Block Diagram for the Temperature Control in the Conditioned Space.....	59
<b>Figure 29:</b> Simulink Results of the Temperature Controller for the Conditioned Space.....	59

<b>Figure 30:</b> Block Diagram to Incorporate the Temperature Controller to the SAACS Prototype.....	62
<b>Figure 31:</b> Block Diagram for the Flow Rate Controller Developed by Meléndez ....	64
<b>Figure 32:</b> Modified LabVIEW Subroutine to Implement the Proposed Temperature Controller.....	65
<b>Figure 33:</b> Actual temperature vs. Desired Temperature Setpoint in the Conference Room.....	66
<b>Figure 34:</b> Control Signal to Reach the Setpoint .....	66
<b>Figure 35:</b> Average Outdoor Temperature Profile Used for the SAACS Performance Tests.....	68
<b>Figure 36:</b> Average Conditioned Space Humidity Profile Used for the SAACS Performance Test .....	68
<b>Figure 37:</b> Thermal Stratified Tank Temperature Profile without the Temperature Controller.....	70
<b>Figure 38:</b> Thermal Stratified Tank Temperature Profile with the Temperature Controller.....	70
<b>Figure 39:</b> Comparison of Outdoor Temperature and the Conference Room Temperature Controlling the Temperature .....	71
<b>Figure 40:</b> Coefficient of Performance (COP) for the Test Performed using the Temperature Controller .....	72
<b>Figure 41:</b> Average Cooling Load from the Absorption Machine .....	74
<b>Figure 42:</b> Overall SAACS Efficiency under the Temperature controller .....	74

## List of Tables

<b>Table 1:</b> Channel Assignment for Output Relays (SCXI-1163) Module .....	22
<b>Table 2:</b> Channel Assignment for 1 <sup>st</sup> SCXI-1100 module. (Type-T) Thermocouples.....	22
<b>Table 3:</b> Channel Assignment for the 2 <sup>nd</sup> SCXI-1100 module. (Voltage and Current type sensors) .....	22
<b>Table 4:</b> Channel Assignment for SCXI-1180. (Analog Outputs) .....	22

# Chapter 1

## Introduction

### 1.1 Solar Air Conditioning Systems

The usage of electricity in air conditioning systems has increased in the past decades [1]. This usage has been limited due to the scarceness of the natural resources. Possibilities of using solar energy have been widely suggested in many countries during many years as an alternative for this problem [2]. Solar-assisted air-conditioning systems using absorption chillers are one of the most appealing new technologies proposed. Solar absorption cooling systems have been installed in different parts of the world to evaluate their feasibility and performance [3], [4]. The first Solar Assisted Air Conditioning System (SAACS) prototype for the Caribbean has been installed in Cabo Rojo, Puerto Rico [5]. The SAACS Prototype consists of a 66 flat plate solar collector array with 115.4 m<sup>2</sup> of selective surface area, a 35 kW single-effect lithium-bromide absorption chiller, a 84 kW cooling tower, a 50 kW auxiliary hot water boiler, a 5700 liter storage tank equipped with flexible stratification manifolds, and a 1800 l/hr air-handling unit. All these works have proven the feasibility of using solar absorption cooling systems. Although the SAACS at Cabo Rojo includes an automatic control using the LabVIEW<sup>®</sup> software [6], some improvements could be accomplished by developing a temperature controller that will operate the chiller under multiple load conditions.

## 1.2 Objective and Contributions

The objective of this research is to design and implement a temperature controller to regulate the temperature of a conditioned space. To regulate the conditioned space temperature, it is necessary to vary the chilled water flow rate, this is the main focus of this thesis. The SAACS prototype has been designed for human comfort and energy efficiency. Here, the designer must deal with temperature as a control parameter, which can have a marked effect on the control objective of maintaining comfort in the conditioned space.

To develop the temperature controller, it is necessary to generate the data required and identify a dynamical model for the plant to be controlled (the conditioned space). The temperature controller will operate the absorption machine at partial load.

The hypothesis is based on the assumption that by controlling the flow in the chilled water loop, we shall attempt to optimize the usage of the available energy in the storage tank. Demonstrating the truthfulness of this assumption, we will provide an increment of the operation hours of the SAACS prototype without penalties in the system's performance.

In addition, this research will study the application of the system identification theory to absorption systems, considering them as "black box" models. To analyze this, a discrete-time state-space model for the absorption machine is developed. The resulting model will provide the base to analyze the absorption machine for simulation and prediction purposes.

### 1.3 Thesis Outline

This thesis is divided into six chapters. Chapter 2 presents previous work on absorption chiller dynamic modeling, the system modeling and parameter estimation of absorption chillers, temperature control of HVACs, and Identification of simple process models for control purposes. Chapter 3 presents a description of the SAACS prototype, the Data Acquisition System, and the experimental approach utilized during this research. Chapter 4 deals with the system modeling and parameter identification used to describe the LiBr/H<sub>2</sub>O single-effect absorption chiller and the conditioned space model. Both models are validated with experimental data. Chapter 5 covers the temperature controller design and its implementation on the SAACS prototype. The simulations are developed using the Matlab<sup>®</sup> and Simulink<sup>®</sup>. The implementation was based on the existing SAACS control and monitoring station developed by Meléndez [6]. Finally, Chapter 6 gives conclusions and recommendations on this research.

## Chapter 2

### Previous Work

This chapter addresses previous research efforts on absorption chiller dynamic modeling, system modeling and parameter estimation of absorption chillers. In addition, temperature control in air conditioning systems as well as the identification of simple process models for control purposes are also reviewed.

#### 2.1 Absorption Chiller Dynamic Modeling

In the development of the solar cooling technology, absorption chillers are the most popular. They have been regarded as most suitable option for this technology because they are compact, reliable and can be easily integrated into existing systems. The feasibility of absorption chillers powered by solar energy has been thoroughly discussed in the literature [5], [7]. The long-term operation of a solar-assisted absorption air conditioning system has also been proven by a system located at Sacramento, California, which has been in operation for more than eleven years [8]. The system located at Cabo Rojo, Puerto Rico has been in operation for almost six years and was the basis for a complete investigation [6].

Mathematical models for the behavior of the absorption cycle have been developed for both configurations, Ammonia-Water ( $\text{NH}_3/\text{H}_2\text{O}$ ) and Water-Lithium

Bromide (H<sub>2</sub>O/LiBr) [9], [10]. These models are based on internal parameters of the absorption machine and the solutions inside. Generally, the internal parameters of the absorption machine are not available for measurement, thus hindering the development of a control algorithm based on these models. To illustrate this, the model provided by Sayigh is presented [9]. The block diagram for this absorption cycle is given below

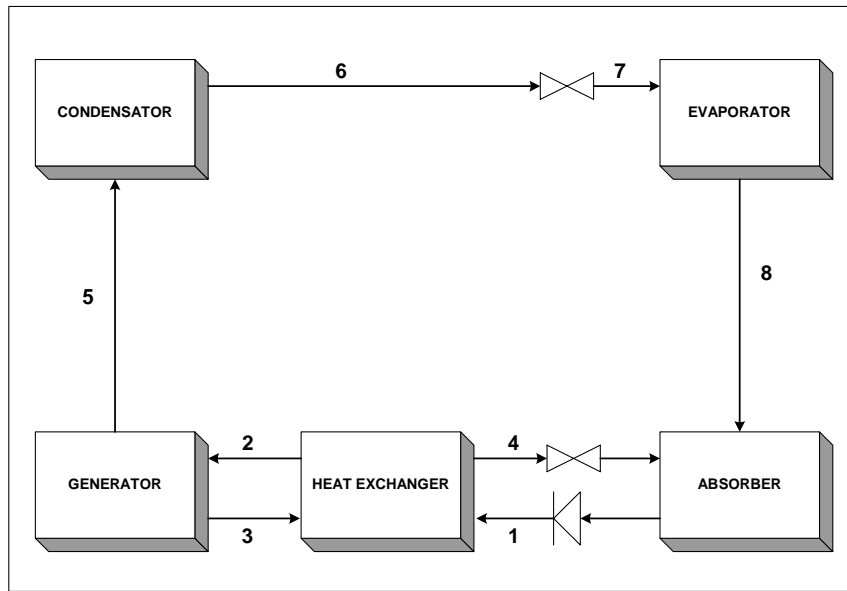


**Figure 1:** Simple Block Diagram of Water-Lithium Bromide Single Effect Absorption Cycle [9]

According to Sayigh [9], the equations are derived separately for each stage of the cycle, with  $\dot{m}_i$  ( $i=1,2,\dots,n$ ) being the mass flow rate and  $x_i$  ( $i=1,2,\dots,n$ ) its corresponding concentration for their specified stage. For the generator, the mass balance equation is

$$\begin{aligned} \dot{m}_2 &= \dot{m}_5 + \dot{m}_3, \text{ flow into generator} \\ x_2 \dot{m}_2 &= x_5 \dot{m}_5 + x_3 \dot{m}_3, \text{ for lithium bromide concentration} \end{aligned} \quad (1)$$

Assuming the flow in 5 is pure water vapor, then  $x_5=0$  so that

$$\frac{x_2}{x_3} = \frac{\dot{m}_3}{\dot{m}_2} \quad (2)$$

$$\dot{m}_2 = \left( \frac{x_3}{x_3 - x_2} \right) \dot{m}_5$$

From the energy balances, it is obtained a relationship between the internal and external variables affecting the cycle's performance.

For the heat exchanger, the energy balance equation is given by

$$h_2 = \frac{\dot{m}_3}{\dot{m}_2} (h_3 - h_4) + h_1 \quad (3)$$

where  $h_i$  ( $i=1,2,\dots,n$ ) represents the enthalpy for that specified thermodynamic stage

The external input variables are accounted for in the generator and evaporator energy balances as

$$Q_{gen} = \dot{m}_3 h_3 + \dot{m}_5 h_5 + \dot{m}_2 h_2 = \dot{m}_5 \left[ \left( \frac{x_3}{x_3 - x_2} \right) (h_3 - h_2) + (h_5 - h_3) \right] \quad (4)$$

$$Q_{evap} = \dot{m}_5 (h_8 - h_6) \quad (5)$$

The last equation describes the condenser heat  $Q_c$  and is given by

$$Q_{cond} = Q_{gen} + Q_{evap} \quad (6)$$

From these equations, it can be seen that the dynamical equations that describe the system operation are nonlinear and appear in terms of the internal concentrations, the loop enthalpies, and the internal mass flow rates of the water vapor out of the generator

In the development of dynamic models of absorption machines, it is natural that the dynamics characteristics should be taken into account in its model design and control. Many studies of the dynamic characteristics of absorption systems have been reported. In 1981, Van Hattem and Dato reported the simulation of a full solar air conditioning system using flat-plate solar collectors, two storage tanks, and a Water-Lithium Bromide absorption machine [11]. In 1982, Anand, et. al, developed a transient analysis with simulations of the absorption cycles based on assumptions of their internal parameters [12]. In 1994, Jeong, et. al, also developed computer simulations on the performance of absorption machines based also on parameters assumptions [13].

In 1995 Zhuo modeled a small-scale absorption system both with lumped and distributed parameter model in the heat transformer [14]. In 1997 Stephan and Schmitt studied in detail the dynamic characteristics of an ammonia-water absorption chiller [15]. They assumed ideal control systems including electronic throttle valves and level meters in the heat transformer.

In 1997, Hernández studied the thermodynamic performance of a single-effect absorption system in Puerto Rico, alone and coupled to liquid and solid-desiccant based dehumidification systems [16]. The absorption system was powered by high performance flat-plate solar collectors and different cooling load conditions were considered in his study. The modeling for the absorption system was based on

performing heat and mass balances on each of its components, while the liquid-desiccant based dehumidification system was simulated using a cooling tower effectiveness model. The model developed by Hernández was the basis for the design of the absorption system used in the SAACS prototype located at Cabo Rojo.

In 1998, Hammad and Zurigat described the performance of a solar cooling unit located at the University of Jordan [17]. In 2001 Chow, et. al, derived a system-based Artificial Neural Network (ANN) model of direct fired double effect absorption machine system [18]. They also discussed a new concept of integrating neural network and genetic algorithms in the absorption system dynamic modeling.

In 2002 Alva evaluated the system's performance of an air-cooled absorption machine through computer simulations [19]. The air-cooled absorption machine was coupled to an array of PCM solar collectors with a phase change material incorporated. The obtained model for this absorption machine was based on developing heat and mass balances on each component of the system, including solar collectors, thermal storage tank, the air-cooled condenser, and the air-cooled absorber. Alva also made comparisons between absorption air conditioning systems that use a cooling tower instead of air-cooled components. The particular absorption system used lithium bromide and water as the absorbent and refrigerant respectively.

In 2002 Degang Fu, et.al., developed a dynamic model for a small-scale direct-fired LiBr/H<sub>2</sub>O chiller with lumped parameter model [20]. They established dynamic mathematical models of each component, as well as the model of the chiller system. A dynamic simulation software was also developed with FORTRAN and VB languages such that the geometry details, entering cooling and chilled water parameters, gas

consumption rate, as well as the solution circulation rate of the chiller could be specified by the users. Finally, in 2003 Kim et.al., developed the dynamic model of a small-scale solar-driven chiller [21]. They simulated the chiller's transient behavior during the startup, taking into account the initial charging amount of solution and its refrigerant concentration.

As we can see, in the precedents works, the absorption machine modeling has been limited to the study of the dynamic characteristics and the performance of each component. In this research, we will consider the absorption machine as a “black box” considering its input-output response to a specific input. Identifying such a model for the absorption machine will allow to predict the dynamical behavior of the machine for simulation and controller design purposes. To the best of our knowledge, such a model has not been reported elsewhere.

## 2.2 System Modeling and Parameter estimation of Absorption Machines

The system modeling of absorption machines using the system identification theory has been limited due to the lack of equipment capable of measuring internal parameters such as enthalpies and mass flow concentrations. The development of discrete-time state-space models using these parameters has not been a common practice. The following are some studies that can be considered as the initiation of system modeling of absorption machines.

In the early 1980s, a need to do worthwhile “*Chiller Testing*” existed and a method was conceived that focused on testing chillers in the field with sustained machine operation. The use of computers for data acquisition and conditioning of field-

acquired data appeared as an alternative of collecting experimental data and afterwards an analysis of the performance of the chiller was conducted. It was found that the performance of an absorption chiller fluctuated during the operation time due to the always-changing weather and cooling load [22].

In 1994, a paper by Aoyama and Izushi brought one of the first experiments applied to a gas fired single-effect lithium bromide absorption machine. This experiment consisted of varying the mass flow rate of the entering hot water driven the chiller while the dynamic response of the chilled water was monitored. The control for this experiment was controlling the gas consumption rate [23]. The data collected was not used to develop a dynamic model, only they limited their study to analyze the Coefficient of Performance (COP) of the absorption chiller.

In 1996 Haves et. al, presented a case study to the problem of detecting and diagnosing faulty methods via parameter estimation [24]. The paper covered the process of model-based fault detection by describing the use of relatively simple empirical models of a gas-fired absorption chiller energy performance to monitor equipment degradation and control problems. The Cool-Tool<sup>TM</sup> chiller model identification package was used to fit the DOE-2 chiller model to on-site measurements from a building instrumented with high quality sensors. The accuracy with which the chiller model expected to predict performance was assessed from the goodness of fit obtained and the implications for fault detection sensitivity and sensor accuracy requirements were discussed. A case study was described in which the model was applied retroactively to high-quality data collected in San Francisco office building as part of a related project.

In 2001 Priya [25] studied three different absorption chiller models: two were based on pure principles models and the third was based on empirical models. The first principles models were the Gordon and Ng Universal Chiller Model (2<sup>nd</sup> generation), and a modified version of the ASHRAE Primary Toolkit model. The DOE-2 chiller model as implemented in Cool-Tool<sup>TM</sup> was selected for the empirical category. All three models were used to evaluate different modeling approaches for their applicability to model based Fault Detection and Diagnosis (FDD) of vapor compression air conditioning units. The studied models displayed similar levels of accuracy. Of the first principles models, the Gordon-Ng had the advantage of being linear in the parameters, which allows more robust parameter estimation methods to be used and facilitates estimation of the uncertainty in the parameters values. The ASHRAE Toolkit Model had the advantages when refrigerant temperature measurements were also available. The DOE-2 model had the advantages when very limited data was available to calibrate the model, as long as one of the previously identified models in the CoolTool<sup>TM</sup> library matched the performance of the chiller.

### 2.3 Temperature Control of HVACS Systems

Models for chilled water HVAC systems have been widely discussed in the literature and can be derived from mass and energy balances relations [26]. Argüello developed the models to be presented next. These equations describe the dynamic behavior of the temperature of the supply air, the temperature of the conditioned space, and the humidity of the conditioned space.

$$\begin{aligned}
\dot{T}_{cs} &= \frac{f}{V_s}(T_{sa} - T_{cs}) - \frac{h_{wv}f}{C_p V_s}(W_{sa} - W_{cs}) + \frac{4}{C_p V_s}(Q_0 - h_{wv}m_o) \\
\dot{W}_{cs} &= \frac{f}{V_s}(W_{sa} - W_{cs}) + \frac{m_o}{\rho V_s} \\
\dot{T}_{sa} &= \frac{f}{V_{he}}(T_{cs} - T_{sa}) + \frac{f}{4V_{he}}(T_o - T_{cs}) - \frac{fh_w}{4C_p V_{he}}[(W_o + 3W_{cs}) - 4W_{sa}] - \frac{6000}{\rho C_p V_{he}}\dot{m}
\end{aligned} \tag{7}$$

where

$T_{cs}$	=	Temperature of cooling space
$T_{sa}$	=	Temperature of supply air
$T_o$	=	Outdoor air temperature
$W_{cs}$	=	Humidity of cooling space
$W_{sa}$	=	Humidity of supply air
$W_o$	=	Outdoor Humidity
$m_o$	=	Moisture load
$V_s$	=	Volume of thermal space
$V_{he}$	=	Volume of heat exchanger
$h_{wv}$	=	Enthalpy of water vapor
$h_w$	=	Enthalpy of water
$f$	=	Volumetric flow rate of supply air
$\dot{m}$	=	Chilled water mass flow rate
$C_p$	=	Specific heat
$Q_o$	=	Sensible heat load
$\rho$	=	Air mass density

Using this model, chilled water flow control for temperature control in the conditioned space can be achievable. Argüello developed a control system using state observers to determine unmeasured parameters and developed a control system for a system whose dynamics are describes by this model structure.

In 1991 Federspiel described a concept for controlling HVAC systems where the performance of the system is tuned to the user's specification based on the user's thermal sensation rating and a model of the thermal sensation [27]. By adjusting the

parameters of the model, the controller learns the conditions which will make a specific user comfortable. The parameters of the model were estimated with a recursive least squares algorithm. A computer simulation based on the calibration of an actual system that uses a PI controller design demonstrated the concept and showed how the system performance was improved by parameter estimation.

In 1996 Rentel developed a non-linear controller using a Plant-Observer-Decoupling law, the results were tested through simulations, reaching the expected results of noninteraction between the temperature and relative humidity in the cooling space [28]. The dynamic behavior of the air conditioning system shown in equation (7) was redefined and given by the state-space equations of the following type

$$\begin{aligned}\dot{\mathbf{x}} &= f(\mathbf{x}) + \sum_{i=1}^m g_i(\mathbf{x})u_i \\ y &= h_i(\mathbf{x}) \quad 1 \leq i \leq p\end{aligned}\tag{8}$$

If the state vector  $\bar{x}$  belong to an open set  $U \in \mathfrak{R}^n$ , then the functions  $h_i$   $1 \leq i \leq p$  are real value functions defined on  $U$ , and  $f, g_1, g_2, \dots, g_m$  are  $\mathfrak{R}^n$  valued mapping defined on  $U$ . The class of description in Equation (8) describes a large number of physical systems of interest in many engineering applications, including the air conditioning system.

#### 2.4 Identification of Simple Process Models for Control Purposes

“Identification for control” in industrial practice most often means that a simple process model with, two three parameters are adjusted to a step response [29]. These

simple models are then used to tune PI and possibly D-parameters in a classical controller.

Simple process models of the kind Static Gain ( $K$ ) plus Time Constants ( $\tau$ ) plus Time Delay ( $T_d$ ) can be considered from a system identification perspective. The recent research area of “Identification for Control”, e.g. [30], [31], [32], has produced many interesting results around the interplay between model estimation and control design.

Despite the fact that many of the components comprising an HVAC system are most accurately modeled as nonlinear distributed parameter systems, in 1996 Federspiel [33], showed that the low order linear transfer function model

$$G_p(s) = \frac{K e^{-sT_d}}{(s + p_1)(s + p_2)} \quad (9)$$

can be used for designing the classical local loop controllers (e.g. PI controller). This research proposes the use of this transfer function model to identify the conditioned space in the SAACS prototype.

## Chapter 3

### SAACS Description and Data Acquisition System

In this chapter, the description of the SAACS prototype utilized in this research is presented and the data acquisition system utilized to collect the experimental data is also described. Finally, the approach of the experiment performed to collect the experimental data is shown and explained.

#### 3.1 SAACS Prototype Description

The SAACS prototype is located at the National Fish and Wildlife Service, Cabo Rojo facilities. This prototype consists of a series of interconnected components or subsystem. The components of the SAACS prototype are: a 66 flat plate solar collector array with 115.4 m<sup>2</sup> of selective surface area, a 35 kW single-effect lithium bromide absorption machine, an 84 kW cooling tower, a 50 kW auxiliary hot water boiler, a 5700 liter storage tank equipped with flexible stratification manifolds, and a 1800 l/hr air-handling unit. Figure 2 shows a schematic diagram of the SAACS prototype used for this research.

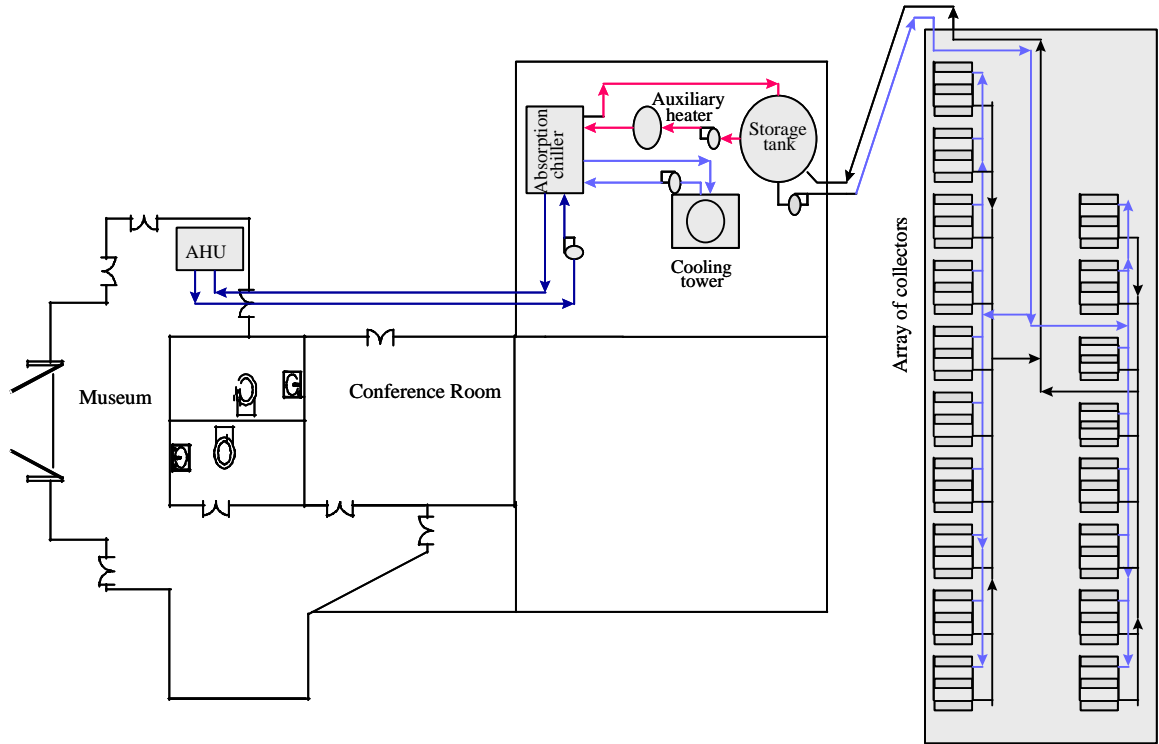


**Figure 2:** Schematic Diagram of the SAACS Prototype Located at Cabo Rojo, Puerto Rico [5]

Meléndez [6] divided the SAACS prototype into three subsystems coupled by the thermal storage unit. The first subsystem is the solar collector array with the thermal storage. The second subsystem is the single-effect lithium-bromide absorption machine whose chilled water output is delivered to the Air Handling Unit (AHU). The third subsystem is the building to be cooled. This building consists of the conference room and the museum at the National Fish and Wildlife Service. The experiment approach for this research focuses on the building and the absorption machine. The following is a brief description of these two subsystems.

### 3.1.1 Absorption Machine and Air handling Unit (AHU)

The lithium-bromide absorption machine used in the SAACS prototype requires three water flow loops in order to function adequately [34]. These loops are the heat medium loop, the cooling tower loop, and the chilled water loop. The absorption machine uses the heat medium loop and the cooling tower loop as inputs and the chilled water loop is its output. The heat medium loop is responsible for providing the heat used to power the absorption cycle to separate the refrigerant from the salt solution.

The cooling tower loop is used for two purposes. First, it will condensate the refrigerant prior to the evaporator, in which the cooling effect is produced. Second, it will allow for the resulting solution out of the evaporator to recombine with the salt solution.

The chilled water loop delivers the chilled water to the air handling unit. Figure 3 shows a schematic diagram of the absorption chiller setup including sensors and actuators for monitoring and control purposes.

In the SAACS prototype, this subsystem contains a total of 11 sensors and 8 actuators. The cooling tower loop has two thermocouples to monitor the temperature signals for the inlet and outlet pipes and a flow meter to measure the loop's mass flow rate. The loop has two actuators, the water pump and the cooling tower fan. This loop has no flow control valve, thus the flow is set at its nominal operating state and is just monitored for safety purposes. The chilled water loop also has two thermocouples to monitor the inlet and outlet temperatures and a flow meter to measure the mass flow rate. There is also a feedback signal from its proportional flow control valve. The flow control valve, a water pump and the AHU fan are the actuators for this loop. Finally, the

heat medium loop has a flow sensor and three temperature sensors. The additional temperature sensors in this loop are required due to the auxiliary gas-fired boiler. The first temperature sensor monitors the inlet to the boiler, the second the boiler's outlet as well as the heat medium inlet, and the third the heat medium outlet temperature reading. The actuators in this loop are the water pump, the boiler itself and an On-Off 3-Way valve.

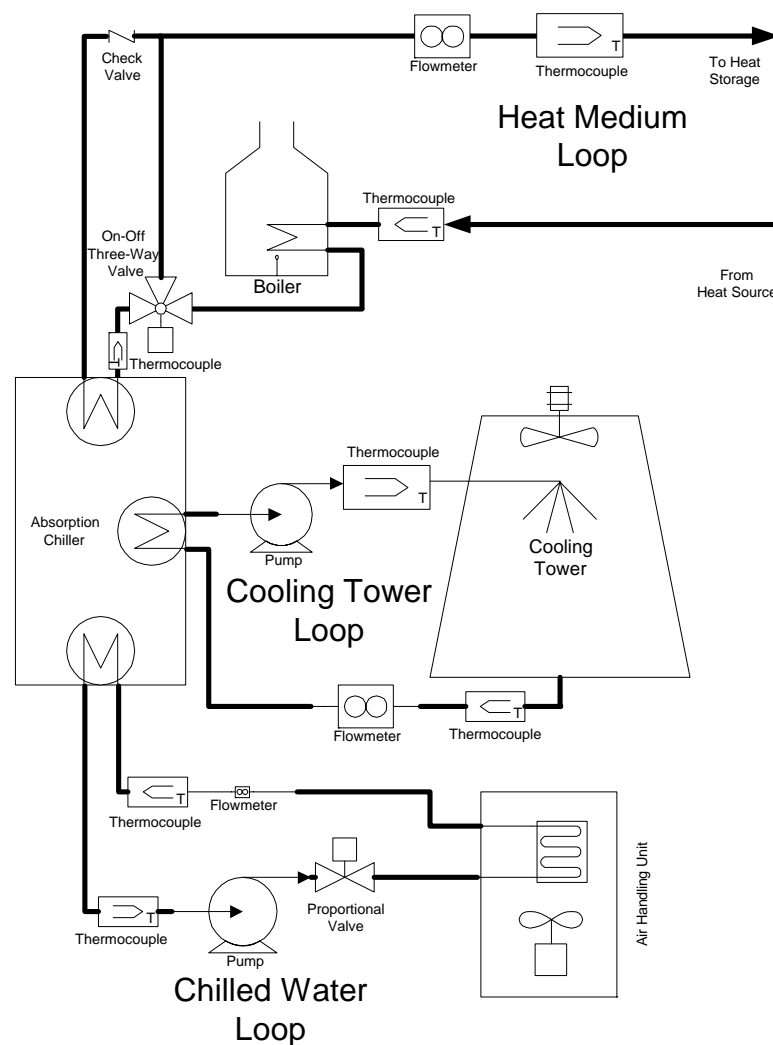


**Figure 3:** Schematic Diagram of the Absorption Machine and the AHU [6]

### 3.1.2 Conditioned Space

The conditioned space that uses the SAACS prototype consists of a conference room and a museum. In order to monitor effectively the temperature and humidity of the conditioned space, a monitoring setup was installed in the site. This monitor includes temperature/humidity conditions in both inlet and outlet ducts of the AHU and temperature/humidity signals of the conditioned space. It also contains outdoor measurements of temperature and humidity. These measurements are used to compare outdoor and indoor conditions of the site for prototype performance. Figure 4 shows a schematic diagram of the conditioned space and its respective sensors.

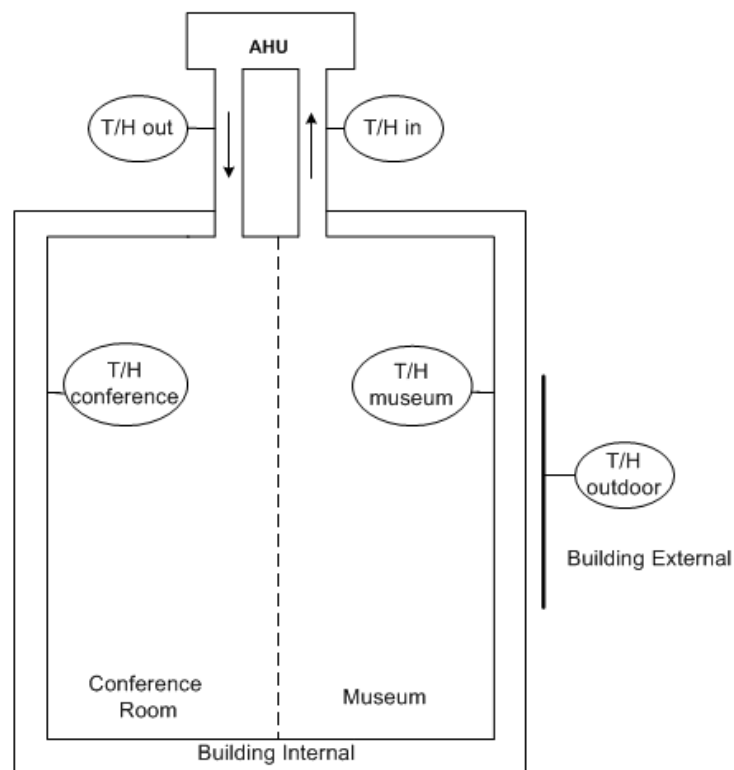


**Figure 4:** Schematic Diagram of the Conditioned Space and its Sensors

## 3.2 Data Acquisition System

The integration of the data acquisition system (DAS) for the purpose of acquiring experimental data is described below. This setup consisted of both hardware and software components since the main operations of the experiment were run from a computer

### 3.2.1 Hardware Configuration

The main components of the hardware configuration for the SAACS prototype consisted of a National Instruments Data Acquisition (NIDAQ) system. This setup contained a PCI-MIO-16XE-10 DAQ board, a SCXI-1000 chassis, 2 SCXI-1100, 1 SCXI 1163R and 1 SCXI-1180 module with 1 SCXI-1302, 2 SCXI-1303 and 1 SCXI-1326 terminal block. The description of these components is given below.

- PCI-MIO-16XE-10 – Multifunction I/O card with 16 single-ended or 8 differential analog input channels at 16-bit resolution, 2 analog outputs at 12-bit resolution, 8 digital 5V/TTL I/O lines and 2 up/down 24-bit counters.
- SCXI-1000 – Chassis that provides power and housing to four SCXI modules. Includes the SCXI bus, which routes analog, digital, timing, and triggering signals between modules and the DAQ board or module.
- SCXI-1100 – 32-channel multiplexer/amplifier with selectable gains and bandwidth settings for configuring the module to condition a variety of

millivolts and volt signals. Allows easy connectivity to thermocouples, voltage and current signals.

- SCXI-1163R – solid-state relay output module with 8 banks with 4 relay output modules each. Each relay can switch up to 240 VAC/VDC at 200mA.
- SCXI-1180 – Feed through panel to extend the I/O signals of the plug-in DAQ board to the front of the SCXI chassis.
- SCXI-1302 – terminal block with 50 screw terminals for use with the SCXI-1180 feedthrough panel in the SCXI-1000 chassis.
- SCXI-1303 – terminal block for use with the SCXI-1100 module. Designed for high-accuracy thermocouple measurements with isothermal construction and a cold-junction sensor installed on the terminal block. Also used for high-accuracy measurements of current and voltage signals.
- SCXI-1326 – High-voltage terminal block with 48 screw terminals for signal connections to the SCXI-1163R module.

This NIDAQ configuration has the capacity of reading 64 analog input channels while providing 32 relay output signals, two analog output signals and two counter I/O signals. The experimental approach for this research required 17 analog input channels, 7 relay output channels, and one analog output channel. The following tables give the channel assignment used during the experiment approach

Name	Description	Device Channel
Pct	Cooling Tower Pump	Port Relay Line 5
Pcw	Chilled Water Pump	Port Relay Line 6
Pgen	Generators Pump	Port Relay Line 7
Fan	Cooling Tower Fan	Port Relay Line 8
AHU	Air Handling Unit	Port Relay Line 9
Boiler	Auxiliary Heater	Port Relay Line 10
3WayChiller	3-Way Valve for Absorption Chiller	Port Relay Line 11

**Table 1:** Channel Assignment for Output Relays (SCXI-1163 module)

Name	Description	Device Channel
Tcrtc	Conference Room Temperature - Thermocouple Reading	Channel 4
Tmtc	Museum Temperature - Thermocouple Reading	Channel 5
Tctti	Cooling Tower Input Temperature	Channel 9
Tctto	Cooling Tower Output Temperature	Channel 10
Tcwti	Chilled Water Input Temperature	Channel 11
Tcwto	Chilled Water Output Teperature	Channel 12
Thti	Auxiliary Heater Input Temperature	Channel 13
Thto	Auxiliary Heater Output Temperature - Chiller Input Temperature	Channel 14
Tcto	Chiller Output Temperature	Channel 15

**Table 2:** Channel Assignment for 1<sup>st</sup> SCXI-1100 module (Type-T Thermocouples)

Name	Description	Device Channel	Sensor Type
Fct	Cooling Tower Flowmeter	Channel 4	Current
Fchw	Chilled Water Flowmeter	Channel 5	Current
Fchill	Absorption Chiller Generator Flowmeter	Channel 6	Current
Tmus	Museum Temperature	Channel 7	Voltage
CWFbk	Chilled Water proportional feedback valve	Channel 23	Voltage
Tconf	Conference Room Temperature	Channel 25	Voltage
Tahuo	Air Handling Unit Output Temperature	Channel 27	Current

**Table 3:** Channel Assignment for the 2<sup>nd</sup> SCXI-1100 module (Voltage and Current type sensors)

Name	Description	Device Channel	Type
CWPropV	Chilled Water Proportional Flow Control Valve	Channel 1	Analog Output

**Table 4:** Channel Assignment for SCXI-1180 (Analog Outputs)

### 3.2.2 Software Configuration

The Data Acquisition System (DAS) described previously was controlled using the LabVIEW<sup>®</sup> (v5.0) software from National Instruments. This software employs an object-oriented programming language called Virtual Instrument (VI) to create Graphical User Interfaces (GUI) for reading inputs and generating outputs. The experimental data was collected using the monitoring station. This monitoring station provides the tools for controlling the different actuators and acquiring the required signals at any established scan interval. Figure 5 shows the front panel of the LabVIEW<sup>®</sup> GUI developed for this research for data acquisition.

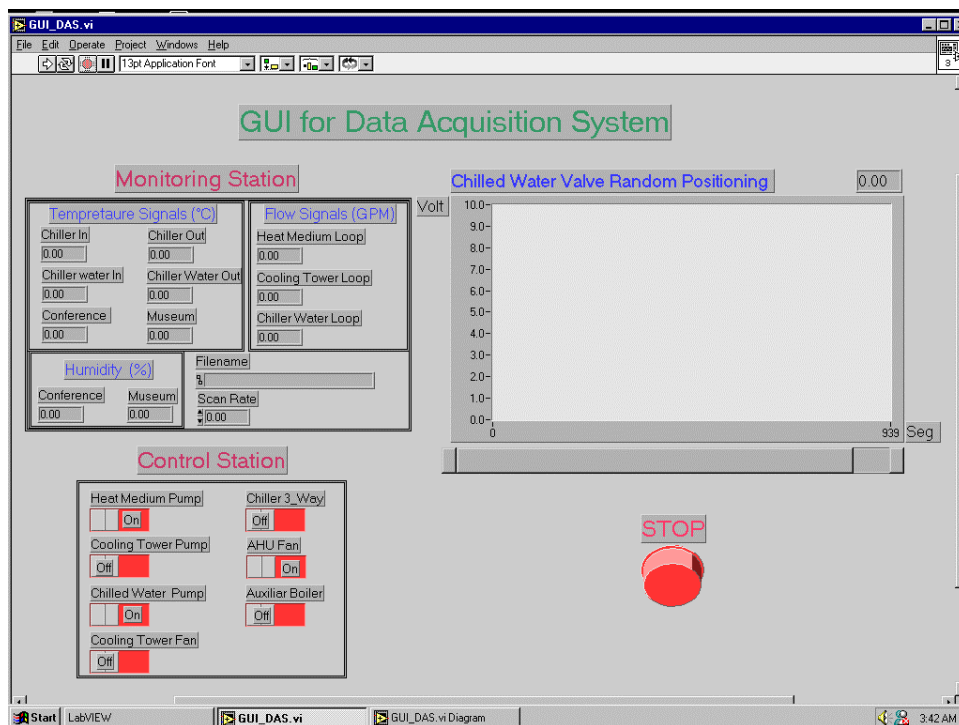


**Figure 5:** GUI for the Data Acquisition

The default screen of the program shows the monitoring station, the control station and the chilled water random positioning waveform graph. In the monitoring station the variables required to develop the system models are displayed. These variables consist of temperature ( $^{\circ}\text{C}$ ), mass flow (GPM) and relative humidity (%) signals. The control station consists of the actuator's output located below of the monitoring station. The chilled water random positioning waveform graph displays the time sequence for the chilled water mass flow rate.

### 3.3 Experimental Approach

During this research, the integration of the data acquisition hardware and software for the purpose of acquiring the required data was accomplished. The acquired data was used to develop estimated models for the absorption chiller and the conditioned space. The experiment was carried out in the SAACS prototype at the Cabo Rojo facilities. A schematic illustration of the experimental setup is shown in Figure 6.

To collect the data for the identification of the absorption chiller subsystem, the flow rate in the chilled water line was considered as the input. The subsystem outputs were the difference between the inlet and outlet temperatures in the heat medium and chilled water loops, respectively. For the identification of the conditioned space, the data collected considered the flow rate in the chilled water line as the input. The output was the conference room temperature.

The experiment consisted on varying the flow in the chilled water line. This flow was varied by requesting a random opening of the proportional valve every ten minutes. While the flow was varied, the outputs described above were recorded each minute. The data collected during this experiment was used to develop the system modeling of the conditioned space and the absorption chiller.

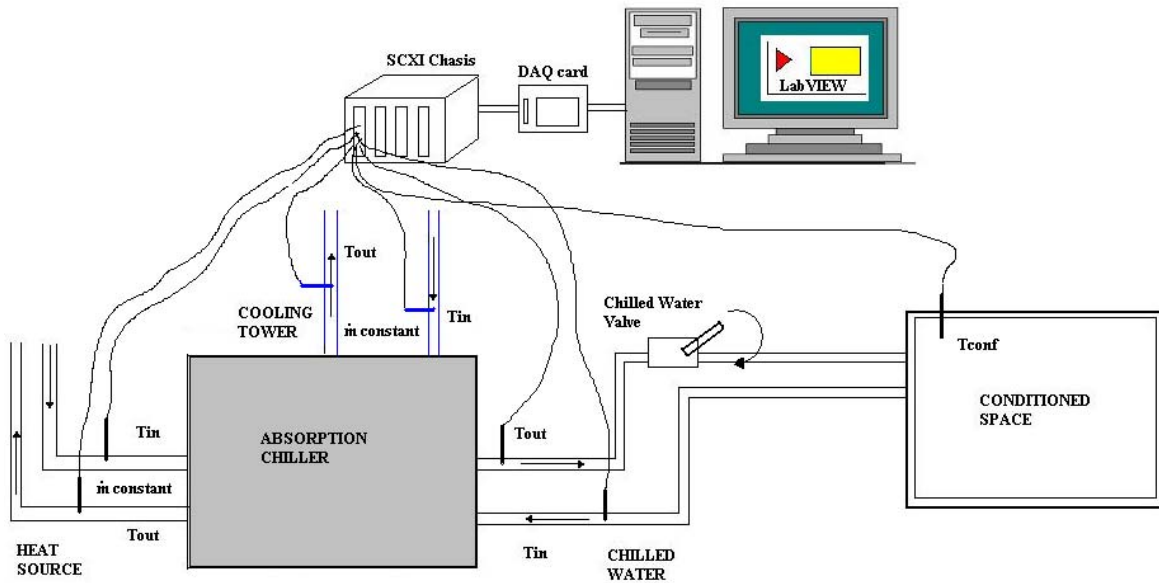


**Figure 6:** Schematic of the Experimental Setup

## Chapter 4

### System Modeling

This chapter addresses the dynamical system modeling of the single-effect LiBr/H<sub>2</sub>O absorption machine and the conditioned space described in the precedent chapter. First, the fundamental system identification and parameter estimation theory is presented. After that, a discrete-time state-space model for the absorption machine is developed. This estimated model is treated as a “black box”. Here the obtained model can be used for simulation and prediction purposes. The second model identified was that for the conditioned space. This conditioned space consists of the conference room and it is treated as a plant represented by a simple process model of the kind static gain plus two time constants and a time-delay. The identification of the conditioned space focuses on the identification for control of a predetermined model. The two identified models are validated and the results of the system modeling are presented and discussed.

#### 4.1 System Identification and Parameter Estimation Theory

The system dynamical model is essential for developing a control system for any given physical process. From this model, it is possible to understand the process behavior, anticipate its response to any given input and develop control structures to regulate the process and make it comply with a set of design objectives. Mathematical

models of physical process can be classified into two broad classes: empirical models known as “*black-box*” models, and analytical models known as “*White-box*” models [35].

*The Empirical models* do not incorporate any kind of prior knowledge of the system. These models are known as “black box” models. Examples of empirical models include polynomial curve fits, and artificial neural networks. An advantage of empirical models is that detailed physical knowledge of the system is not necessary. A disadvantage is that the model is reliable only for operating points within the range of the training data, and extrapolation outside this range may lead to significant error. In order to properly train the model, adequate training data are required; the richer the data, the more accurate the model predictions.

*The Analytical or physical models*, also known as “white-box” models are largely based on the natural laws that describe the phenomena in this case energy and mass conservation principles. Physical models may require less training data, since the model should be valid at all operating conditions for which the assumptions inherent in the model are valid. A disadvantage is that a good understanding of the physical phenomena is necessary for an accurate model, which is not always available. It is nearly impossible to model a system perfectly, and in addition, ‘unmodeled disturbances’ contribute to the inaccuracy of the model. In practice, a model may be partly empirical, and partly based on first principles. These kinds of models are the well-known “grey box” models.

Although mathematical models for the absorption machine and temperature control have been presented in the previous work section, they depend greatly on

several parameters whose values cannot be either measured or vary with operating conditions [36].

In the set of experiments developed under this research, the absorption machine is considered as a “black box” model. The resulting estimated model will have the following form

$$\begin{aligned}\mathbf{x}(k+1) &= \mathbf{A}\mathbf{x}(k) + \mathbf{B}\mathbf{u}(k) \\ \mathbf{y}(k) &= \mathbf{C}\mathbf{x}(k) + \mathbf{D}\mathbf{u}(k)\end{aligned}\tag{10}$$

where  $\mathbf{x}(k)$  is called the state vector,  $\mathbf{u}(k)$  is the input vector, and  $\mathbf{y}(k)$  the output vector.  $\mathbf{A}$ ,  $\mathbf{B}$ ,  $\mathbf{C}$ , and  $\mathbf{D}$  are called the state-space matrices. The model described above, is a set of  $n$  first order linear difference equations that describe the evolution in time of the state variable in response to the input vector  $\mathbf{u}(k)$  while the output vector  $\mathbf{y}(k)$  is measured each sampling time  $T$ . The resulting estimated model of the form of equation (10) for the absorption machine can be used for further research to simulate and predict the absorption chiller behavior when the flow rate in the chilled water line is varied.

#### 4.1.1 “Black Box” Discrete-Time Parameterizations

When there is not knowledge about of internal structure of the discrete-time space model of a dynamic process, it is necessary to search for a linear model that approaches its dynamical behavior. This discrete-time state-space model can be initialized by the well-known subspace identification (ID) methods.

The Subspace ID methods have many attractive features, including their numerical robustness and noniterative features, which are well suited for multivariable

identification. Subspace methods are still geared, either implicitly or explicitly, towards providing accurate one-step-ahead predictions [37].

The conventional subspace ID approach such as, the N4SID method implicitly assumes that the purpose of the model is to provide accurate one-step ahead prediction [35]. This is most apparent when the state-space matrices **A**, **B**, **C**, and **D** are estimated through the least squares method. N4SID are algorithms used to identify mixed deterministic stochastic systems. The algorithms determine state sequences through the projection of input and output data. These sequences take form of outputs for non-steady Kalman filter banks, from which the state-space system matrices are determined. Data bank for one-step ahead Kalman state estimate  $\mathbf{x}_{t+1/t}$  (the next state conditioned to the precedent state) is first created from input/output data. Once this data is created, the state-space matrices are found by solving the following linear least square problem [38]

$$\begin{aligned}\mathbf{x}_{t+2/t+1} &= \mathbf{A}\mathbf{x}_{t+1/t} + \mathbf{B}\mathbf{u}_{t+1} + \mathbf{K}\mathbf{e}_{t+1/t} \\ \mathbf{y}_{t+1} &= \mathbf{C}\mathbf{x}_{t+1/t} + \mathbf{D}\mathbf{u}_{t+1/t} + \mathbf{e}_{t+1/t}\end{aligned}\tag{11}$$

where **K** is the Kalman gain matrix and the vector **e** represents the difference between the measured output and the estimated output. The model minimizes the one step ahead prediction error. In Equation (11), each present value of the output is predicted from the precedent values of the states, the input and the error. The N4SID method will be used as part of the System Identification Toolbox for Matlab<sup>®</sup> to identify the absorption machine.

#### 4.1.2 Discrete-Time Transfer Functions Parameterization

A linear discrete-time transfer function of given structure can be specified by the prediction error method (PEM). The PEM is a standard system identification framework. It calculates the difference between the process output and the one step ahead prediction of the estimated model. The following is a brief description of how the prediction error identification is applied to any particular case.

Suppose that we have collected a data set  $D^N = \{u(1), y(1), \dots, u(N), y(N)\}$  of sampled inputs  $\mathbf{u}(k)$  and outputs  $\mathbf{y}(k)$ . Suppose also that the sampling interval is constant and equal to  $T$ , then a linear system can be described by

$$\mathbf{y}(t) = \mathbf{G}(q)\mathbf{u}(t) \quad (12)$$

Here  $\mathbf{u}(t)$  is the input signal, and  $\mathbf{G}(q)$  is the transfer function from input to output  $\mathbf{y}(t)$ . The symbol “ $q$ ” is a shift operator and can be compared with the “ $z$ ” variable in the Z-transform.

Now, if the transfer function  $\mathbf{G}(q)$  in equation (12) is not known. A parameter vector “ $\theta$ ” can be introduced in its description reflecting this lack of knowledge. In any case the resulting, parameterized model will be described by

$$\hat{\mathbf{y}}(t/\theta) = \mathbf{G}(q, \theta)\mathbf{u}(t) \quad (13)$$

Here  $\mathbf{G}(q,\theta)$  is the transfer function in the selected model structure and  $\hat{\mathbf{y}}(t/\theta)$  is the model output led by the predictor that depends on the unknown parameter vector and past data  $D^{t-1}$ .

From observed data and the predictor  $\hat{\mathbf{y}}(t/\theta)$ , the output error will be

$$\mathbf{e}(t,\theta) = \mathbf{y}(t) - \hat{\mathbf{y}}(t/\theta), \quad \text{with } t=1,2,\dots,N \quad (14)$$

The parameters are then estimated by solving the non-linear least square problem

$$\hat{\boldsymbol{\theta}}_N = \arg \min_{\boldsymbol{\theta}} \sum_{t=1}^N \|\mathbf{y}(t) - \hat{\mathbf{y}}(t/\boldsymbol{\theta})\|_2 \quad (15)$$

The prediction error identification method was used to identify the conditioned space transfer function. The IDGREY object contained in the Matlab<sup>®</sup> System Identification Toolbox is just an especial case of this method and can be utilized to fit the conditioned space model structure to data.

## 4.2 System Modeling Results

For the absorption chiller used in the SAACS prototype, the mathematical model described in Chapter 1 provides good insights into the system's behavior but turned out to be unusable due to unknown or immeasurable parameters such as entropies and enthalpies that vary with operating conditions [34]. Therefore, a "black box" model was developed for this machine to get its discrete-time state-space model. The obtained

model is then validated with experimental data and can be used for simulation and prediction purposes in further research.

In the case of the conditioned space, the proposed model to be estimated was a low order linear model. This model has the commonly used process transfer function models. The input vector will be the chilled water mass flow rate and the output vector will be the temperature in the conference room. This model is validated with experimental data and then used to design the proposed temperature controller.

The data used to obtain these models were acquired in the experimental SAACS prototype system of Cabo Rojo using a sampling interval of 1 minute. The SAACS prototype is automated with several actuators and sensors that are connected to an acquisition and control system based on a desktop computer [6].

#### 4.2.1 Absorption Machine Modeling

The absorption chiller set up described in Chapter 2 contains several input variables that influence its dynamical behavior [34]. The most influential of these variables are the mass flow rates into the heat medium, the cooling tower, and the chilled water loops. In the first two loops, the incoming flow rate should remain within a specified range in order to insure proper operation of the absorption chiller. If the flow rate in the heat medium loop is not met, crystallization of the lithium bromide solution may occur and may render the chiller temporarily useless. On the other hand, while the chiller is operating, the cooling tower must be removing heat from it in order for the absorption cycle to take place. Again, failure to remove the necessary heat can result in crystallization of the lithium bromide solution.

As it can be inferred from above, the only input variable that can be varied would be the mass flow rate in the chilled water line ( $\dot{m}_{cw}(t)$ ). The output variables considered in this test were the difference between the inlet and the outlet temperature in the heat medium loop ( $\Delta T_{hml}$ ) and the difference between the inlet and the outlet temperature in the chilled water loop ( $\Delta T_{cwl}$ ). For the identification of the absorption machine, the test performed used a random generator to vary the signal to the chilled water proportional valve every 10 minutes, allowing the absorption machine reaches a different steady state condition for every value set by the random generator. The sampling interval for this test was 60 seconds.

The method used is based on estimating unknown parameters of a predetermined linear “black box” model structure. This estimate will have the two outputs described previously. Figure 7 presents the experimental data used for the identification of the absorption machine.

The code program was developed using Matlab<sup>®</sup>, basically uses two functions: (i) The first function is the function IDDATA (Y,U,Ts). This function creates data object to be used for identification routines. Y is the output data, U is the input data and Ts is the sampling time. (ii) The second function is the function N4SID (DATA, ORDER). This function estimates a state-space model using the sub-space method. DATA is the data object created with the function IDDATA and ORDER is the order of the state-space model. Both functions are available in the system Identification Toolbox of Matlab<sup>®</sup>.

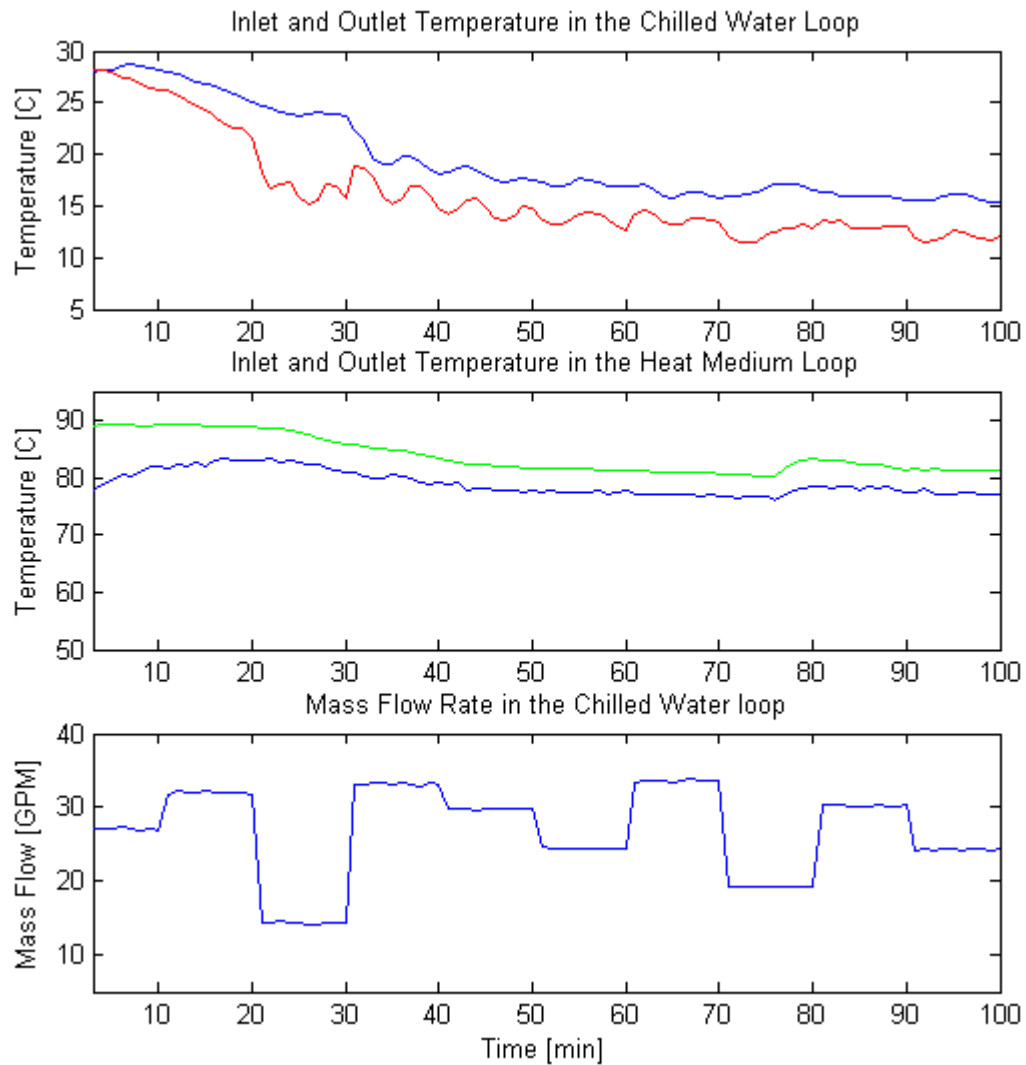


**Figure 7:** Experiment Data Set for Identification of the Absorption Chiller. (a) Inlet and Outlet Chilled Water Loop Temperature, (b) Inlet and Outlet Heat Medium Loop Temperature, and (c) Chilled Water Mass Flow Rate

The program developed with Matlab<sup>®</sup> identified discrete-time state-space models of 2<sup>nd</sup>, 3<sup>rd</sup> and 4<sup>th</sup> order respectively. A comparison between these models is discussed and presented.

The resulting 2<sup>nd</sup> order state-space model for the absorption machine was

$$\begin{aligned} \mathbf{x}(k+1) &= \begin{bmatrix} 0.98548 & -0.034351 \\ -0.12593 & 0.77844 \end{bmatrix} \mathbf{x}(k) + \begin{bmatrix} -0.00084268 \\ -0.0050852 \end{bmatrix} \mathbf{u}(k) \\ \mathbf{y}(k) &= \begin{bmatrix} 15.005 & 1.2526 \\ 7.4174 & -2.2953 \end{bmatrix} \mathbf{x}(k) \end{aligned} \quad (16)$$

The 3<sup>rd</sup> order state-space model for the absorption machine was

$$\begin{aligned} \mathbf{x}(k+1) &= \begin{bmatrix} 0.9866 & -0.0443 & -0.0663 \\ -0.0495 & 0.6256 & -0.6503 \\ 0.2060 & -0.1785 & 0.0630 \end{bmatrix} \mathbf{x}(k) + \begin{bmatrix} -0.00138 \\ -0.01266 \\ -0.01078 \end{bmatrix} \mathbf{u}(k) \\ \mathbf{y}(k) &= \begin{bmatrix} 14.055 & 1.7982 & -0.0575 \\ 7.1229 & -1.9572 & 1.3581 \end{bmatrix} \mathbf{x}(k) \end{aligned} \quad (17)$$

The 4<sup>th</sup> order state-space model for the absorption machine was

$$\begin{aligned} \mathbf{x}(k+1) &= \begin{bmatrix} 1.098 & 0.170 & 0.146 & -0.121 \\ -0.175 & 0.593 & 0.279 & 1.113 \\ -0.064 & -0.026 & 0.576 & -0.539 \\ 0.063 & -0.184 & -0.588 & 0.222 \end{bmatrix} \mathbf{x}(k) + \begin{bmatrix} -0.0018 \\ 0.0037 \\ 0.0013 \\ 0.0044 \end{bmatrix} \mathbf{u}(k) \\ \mathbf{y}(k) &= \begin{bmatrix} 14.166 & -0.6359 & 0.64669 & -0.26861 \\ 6.6678 & 0.21935 & -1.5116 & 2.3066 \end{bmatrix} \mathbf{x}(k) \end{aligned} \quad (18)$$

where  $\mathbf{y}(k) = \begin{bmatrix} \Delta T_{cwl} \\ \Delta T_{hml} \end{bmatrix}$  and  $\mathbf{u}(k) = \dot{m}_{cw}$  (flow rate in the chilled water line)

For these models, the states of the system  $\mathbf{x}(k)$  have no physical meaning. The models were estimated with a set of 100 output/input data samples. Figures 8, 9, and 10

show the fit performed for each model. From these figures, it is seen clearly that each model gives a reasonable description of the system.

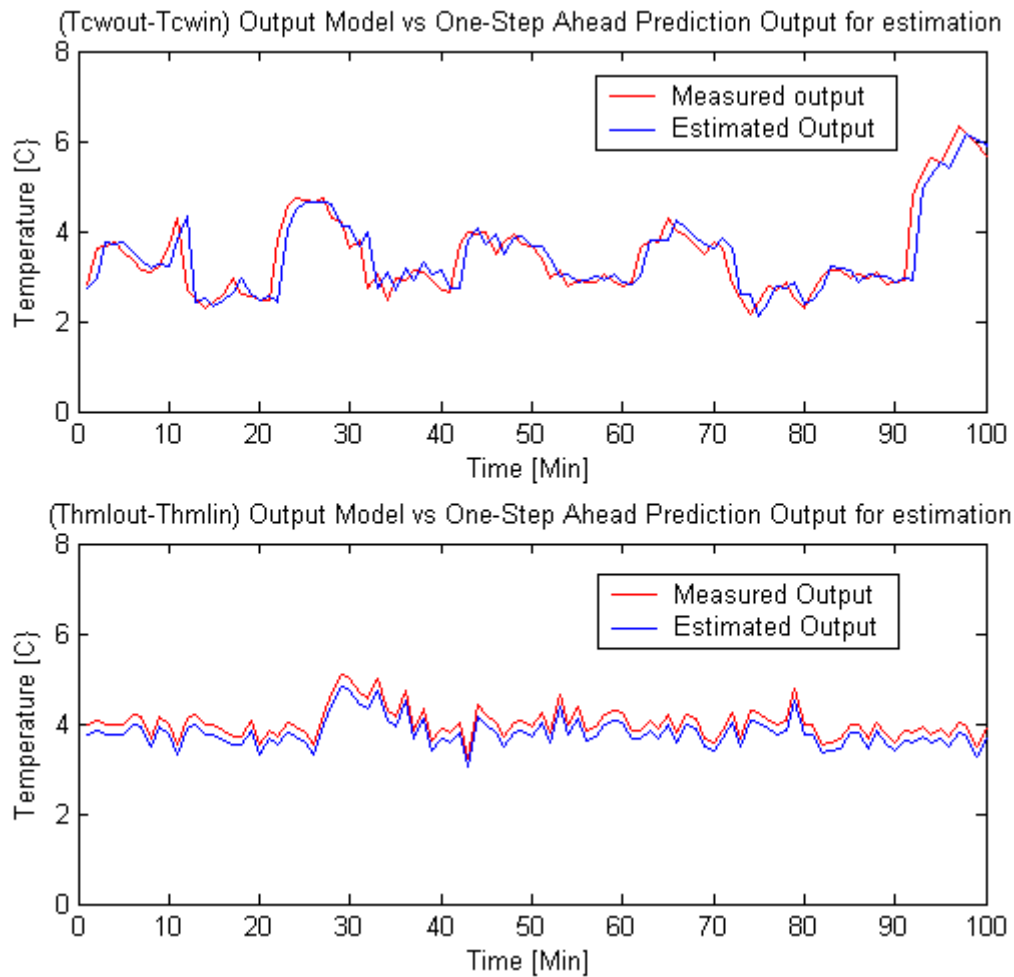


**Figure 8:** Measured and Estimated Output for the 2<sup>nd</sup> order state-space model (a) Inlet and Outlet Chilled Water Loop Temperature and (b) Inlet and Outlet Heat Medium Loop Temperature

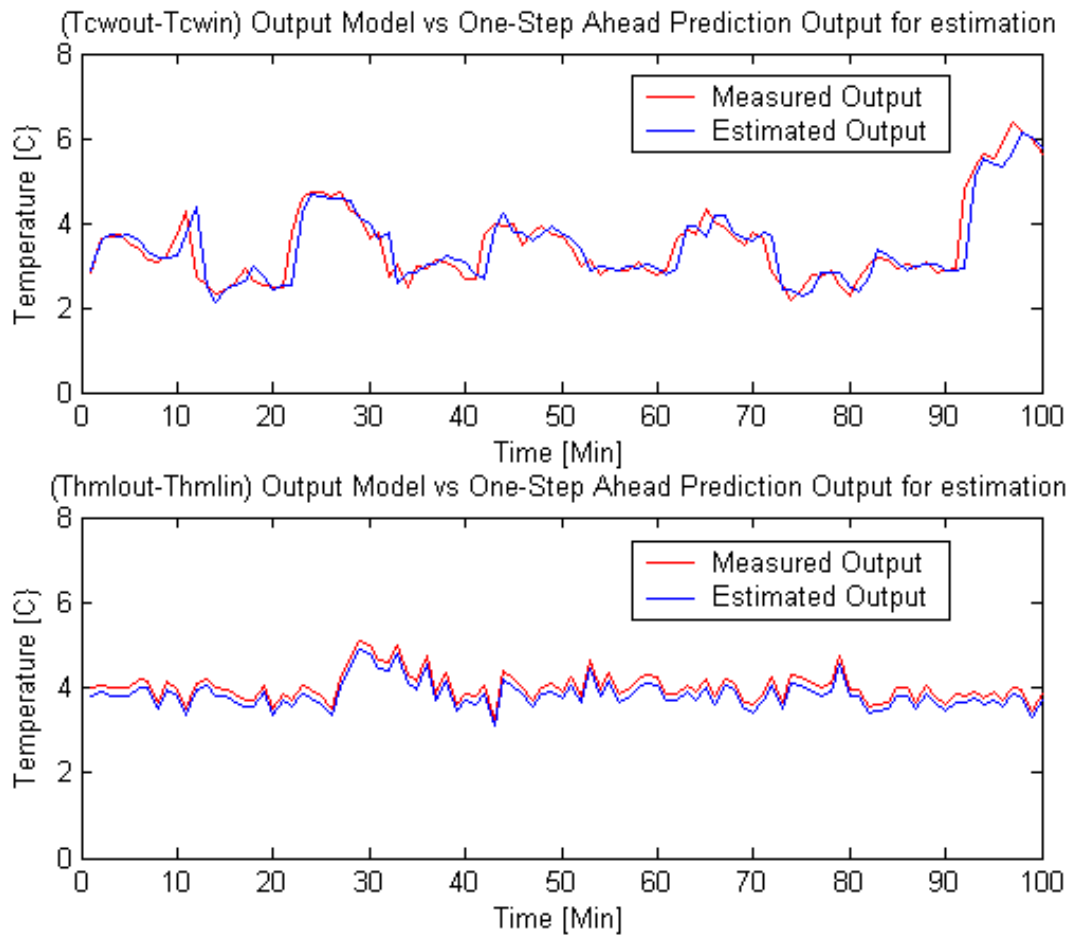


**Figure 9:** Measured and Estimated Output for the 3<sup>rd</sup> order state-space model (a) Inlet and Outlet Chilled Water Loop Temperature and (b) Inlet and Outlet Heat Medium Loop Temperature

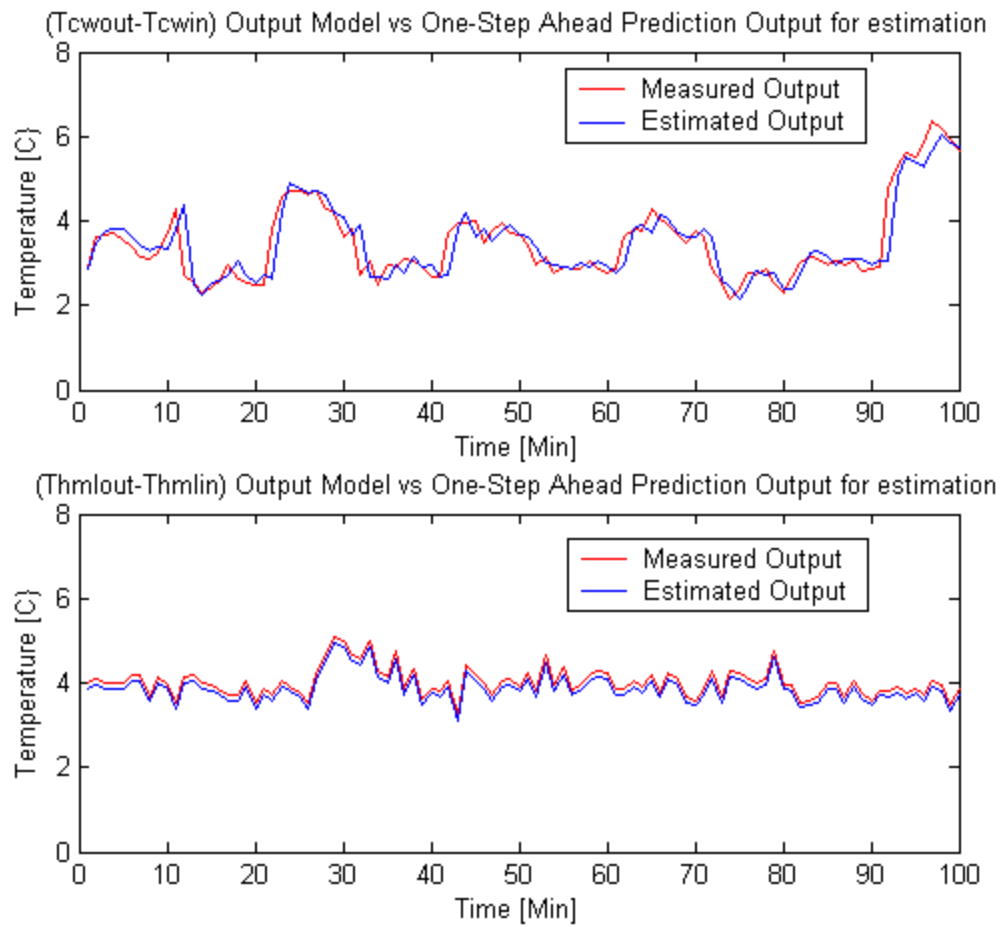


**Figure 10:** Measured and Estimated Output for the 4<sup>th</sup> order state-space model (a) Inlet and Outlet Chilled Water Loop Temperature and (b) Inlet and Outlet Heat Medium Loop Temperature

## Residual Analysis for the Identification of the Absorption Machine Model

A suitable way to determine if the estimated model is a very good model is to develop a residual error analysis. In this analysis, the autocorrelation of the residual errors is presented. Figure 11 shows the residual errors associated with each output data for the 2<sup>nd</sup> order state-space model and their autocorrelation. Figures 12 and 13 show the residual errors and their autocorrelation for the 3<sup>rd</sup> and 4<sup>th</sup> order state-space models respectively. From these figures, it is seen that the residual errors are not correlated and each model has reproduced the information contained in the experimental data.

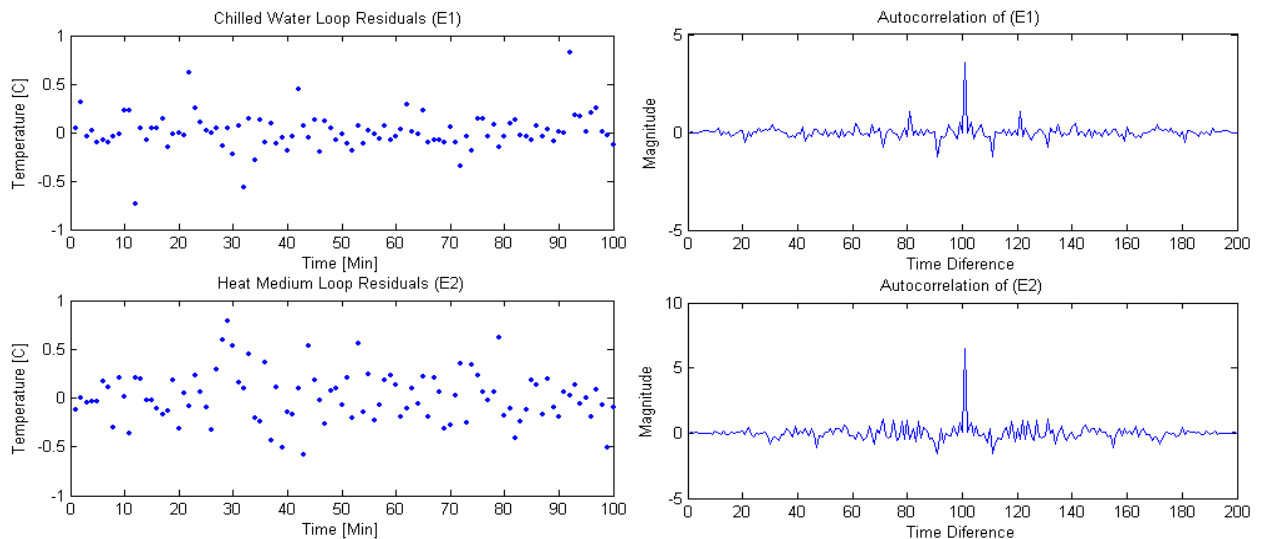


**Figure 11:** Residual Errors for the 2<sup>nd</sup> Order Discrete-Time State-Space Model (Left) and their Respective Autocorrelation (Right)

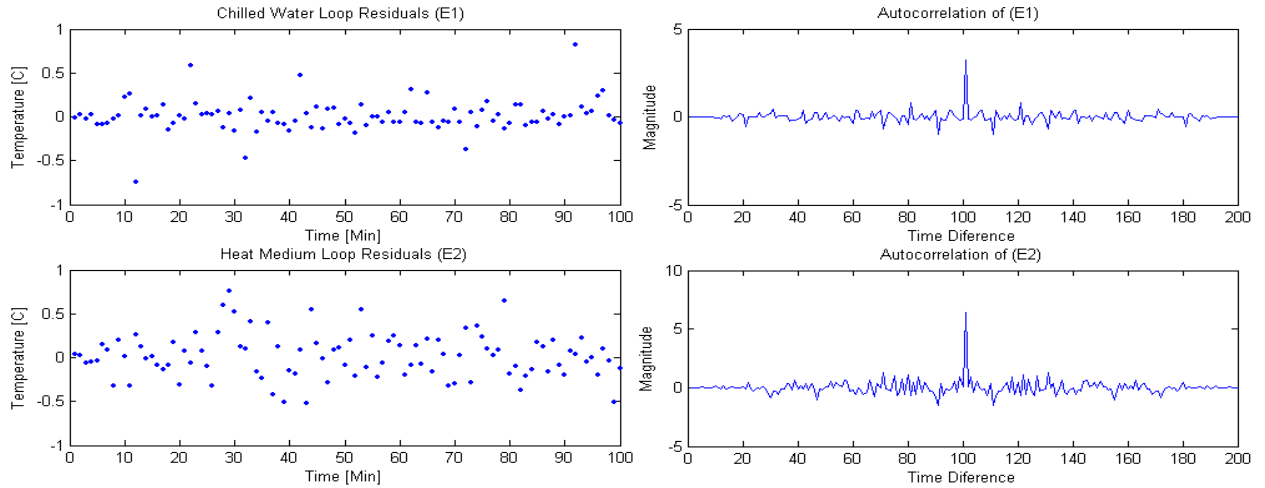


**Figure 12:** Residual Errors for the 3<sup>rd</sup> Order Discrete-Time State-Space Model (Left) and their Respective Autocorrelation (Right)

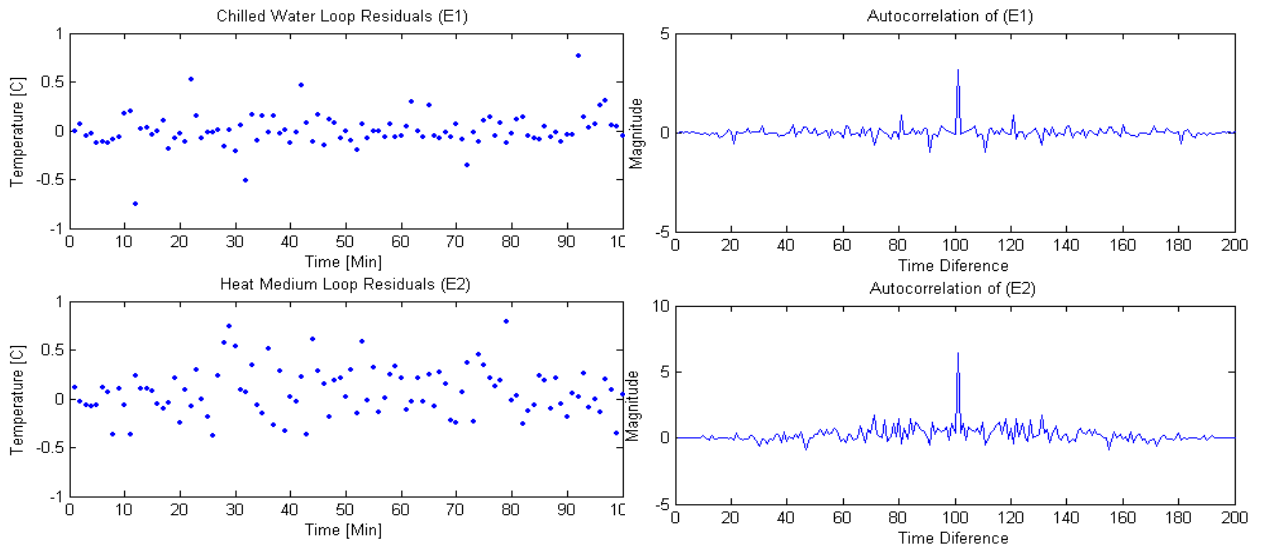


**Figure 13:** Residual Errors for the 4<sup>th</sup> Order Discrete-Time State-Space Model (Left) and their Respective Autocorrelation (Right)

## Validation of the Absorption Machine Model

For the validation stage, a 50 data set was used. Figure 14 shows the validation input data set used.

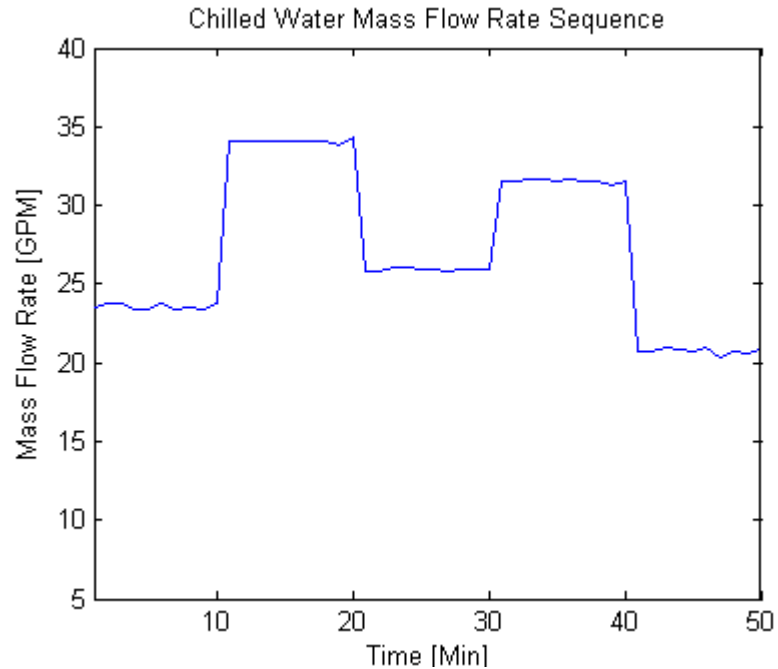


**Figure 14:** Experiment Input Data for Validation of the Absorption Machine

The results of the validation for each model are shown in Figures 15, 16, and 17. Each figure shows the real outputs  $\Delta T_{cwl}$  and  $\Delta T_{hml}$  their estimated outputs  $\Delta T_{cwl}$  and  $\Delta T_{hml}$  for the 2<sup>nd</sup>, 3<sup>rd</sup>, and 4<sup>th</sup> order state-space models. From these plots we can see the closeness of the model and its respective estimated during the validation test.

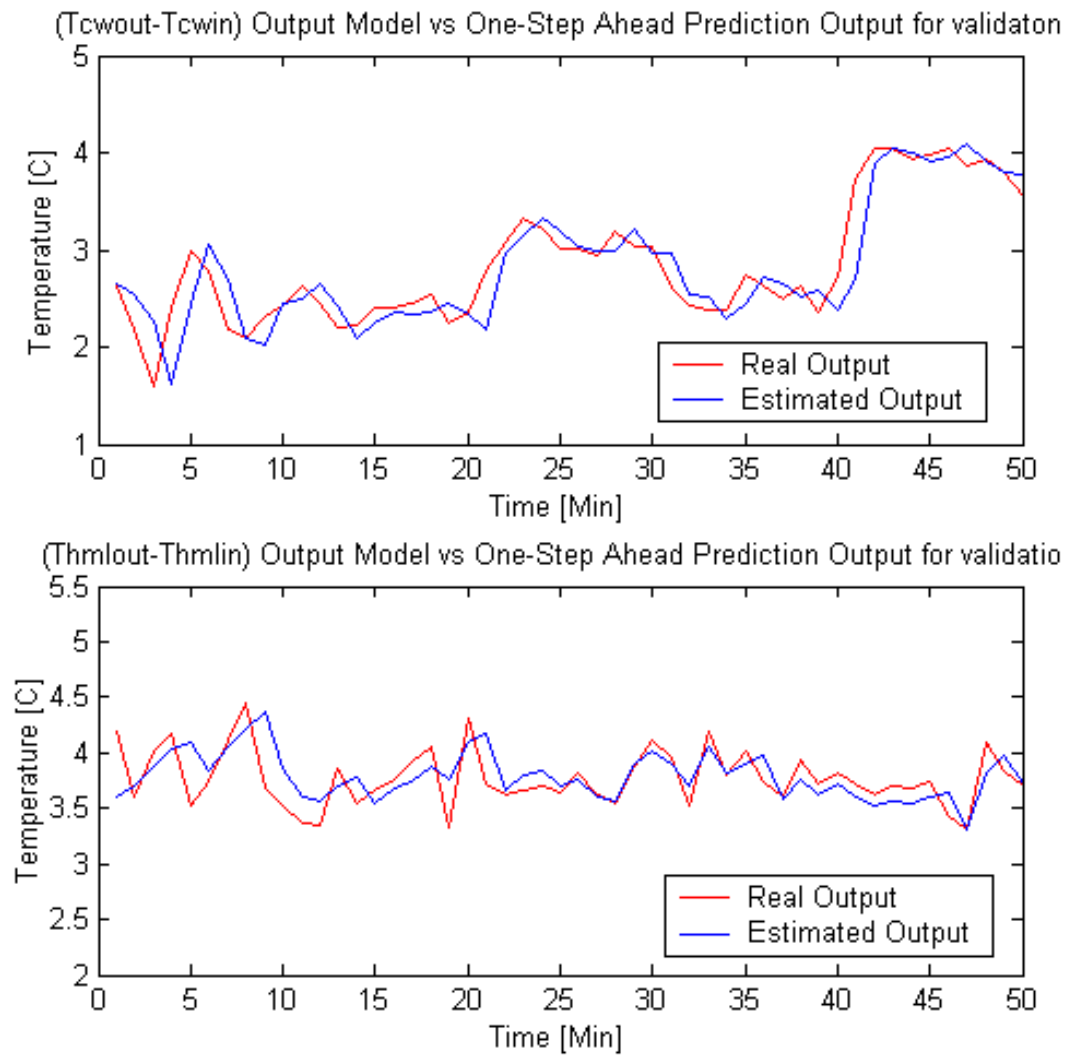


**Figure 15:** Validation Test for the 2<sup>nd</sup> Order Discrete-Time State-Space Model of the Absorption Machine

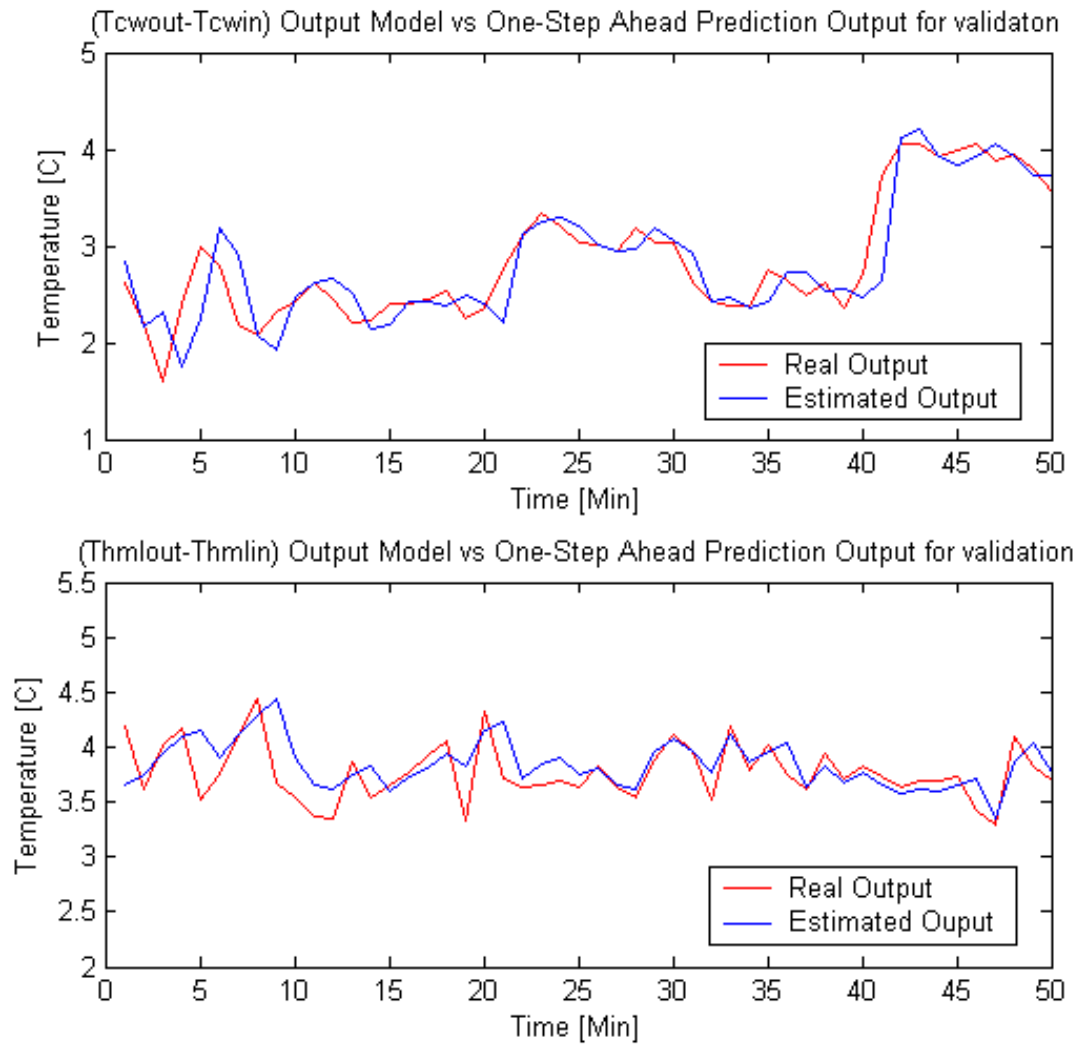


**Figure 16:** Validation Test for the 3<sup>rd</sup> Order Discrete-Time State-Space Model of the Absorption Machine

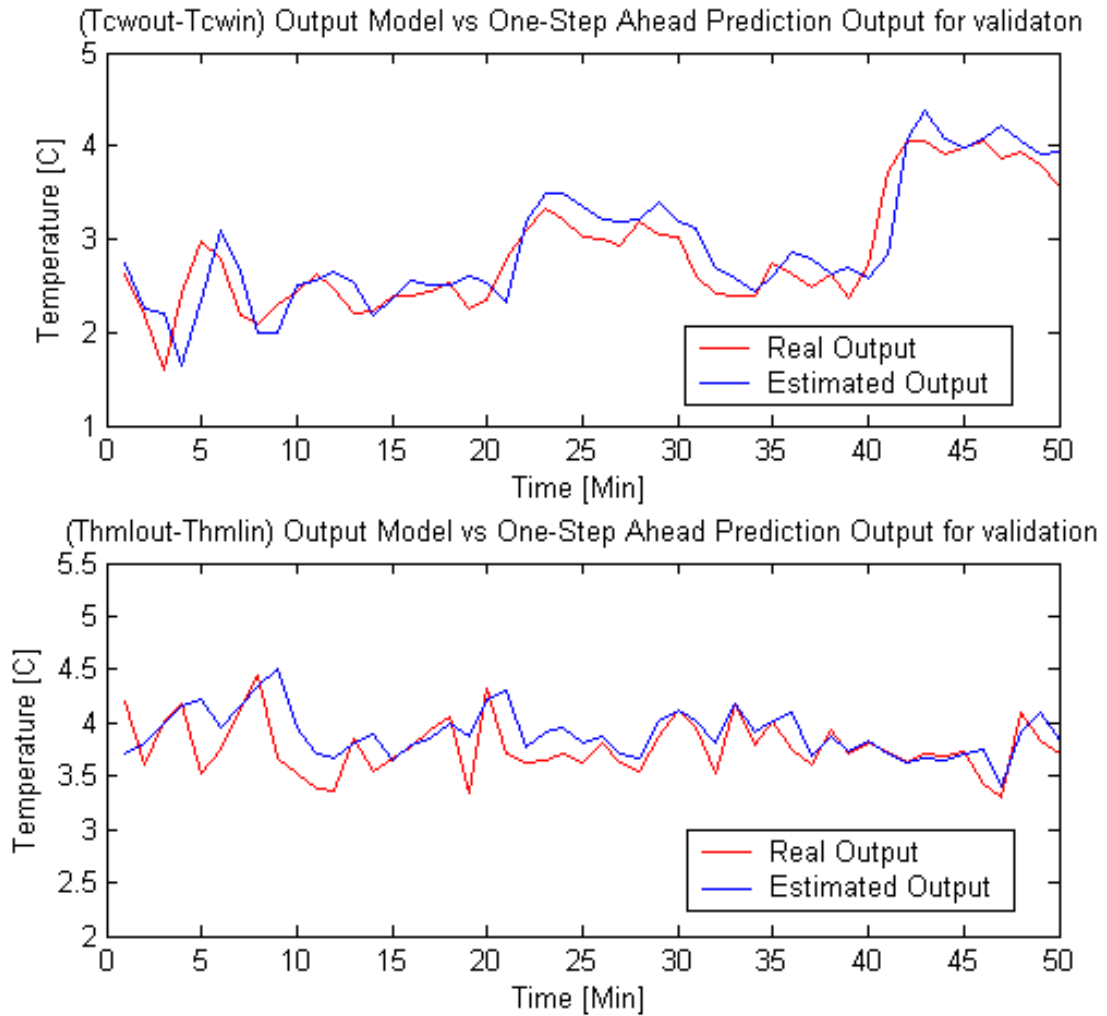


**Figure 17:** Validation Test for the 4<sup>th</sup> Order Discrete-Time State-Space Model of the Absorption Machine

## Residual Analysis for the validation of the Absorption Machine Model

Figures 18, 19, and 20 show respectively the residual errors for the validation data of the 2<sup>nd</sup>, 3<sup>rd</sup>, and 4<sup>th</sup> order model of the absorption machine. In each figure the residual errors and their respective autocorrelation are presented. From these figures, it is seen that the residual errors for each model are not correlated. Figure 21 shows the histogram of the residual errors. Clearly, the histograms present similar behavior for the 2<sup>nd</sup>, 3<sup>rd</sup> and 4<sup>th</sup> order models. The distribution of each histogram approaches to a normal distribution. From these histograms, we can conclude that the error is only due to white noise.

Comparing the three models, it is seen that the 2<sup>nd</sup> order model models the absorption chiller similarly to the 3<sup>rd</sup> and 4<sup>th</sup> order models. To reduce the complexity of the model, the 2<sup>nd</sup> order model is chosen for simulation and prediction purposes in what follows.

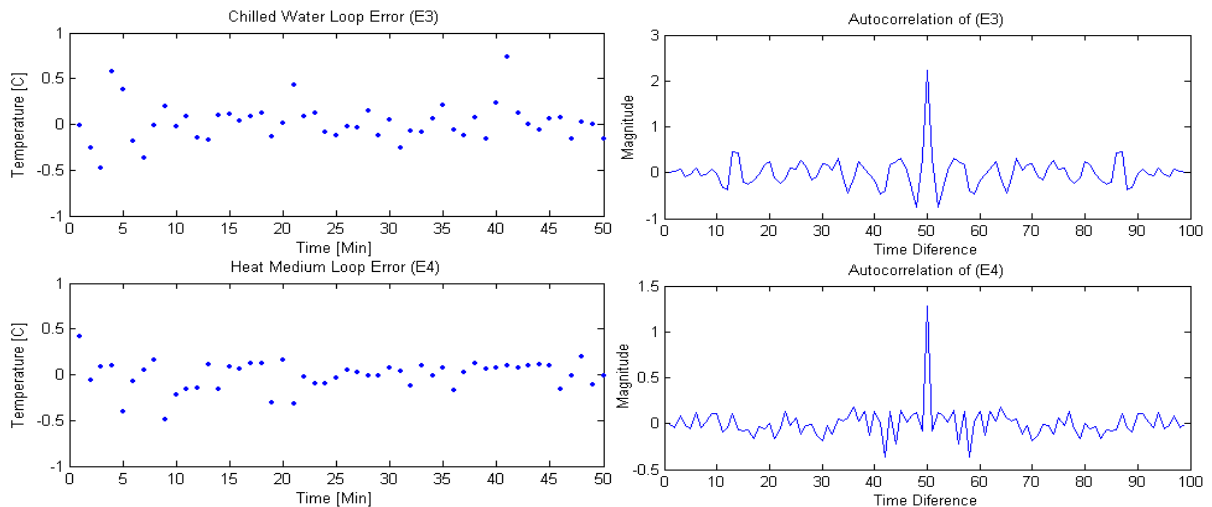


**Figure 18:** Residual Errors of the Validation Test of the 2<sup>nd</sup> Order Discrete-Time State-Space Model (Left) and their Respective Autocorrelation (Right)

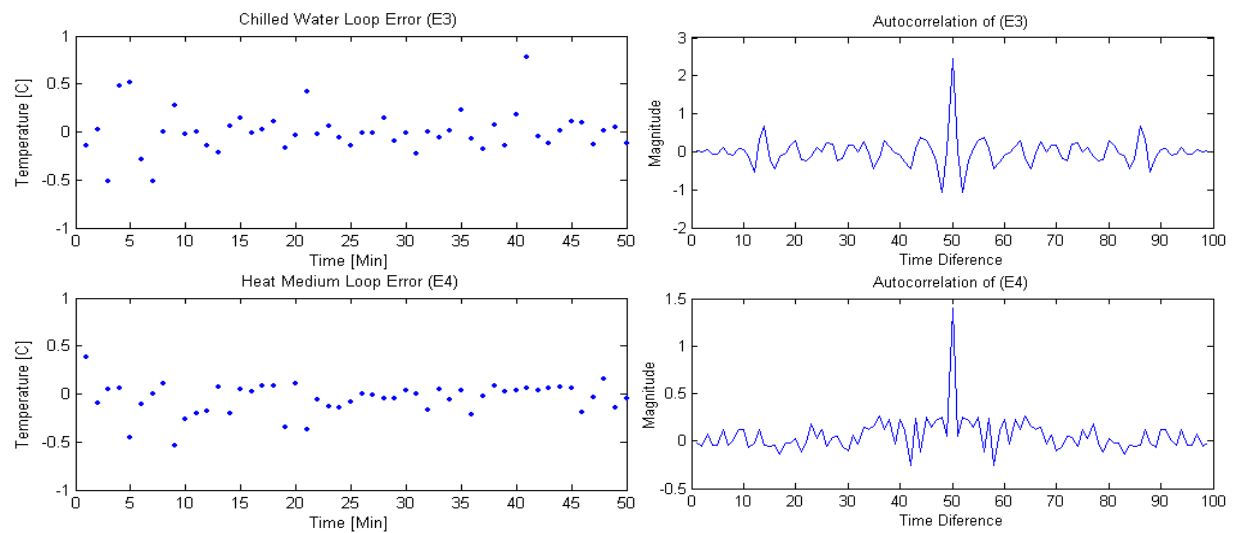


**Figure 19:** Residual Errors in the Validation Test for the 3<sup>rd</sup> Order Discrete-Time State-Space Model (Left) and their Respective Autocorrelation

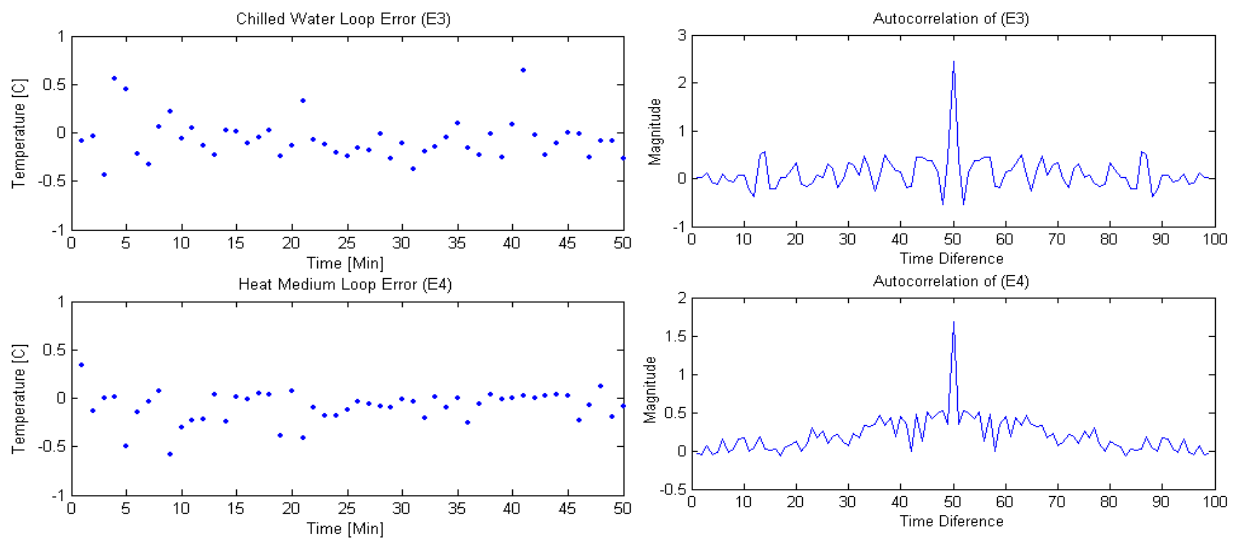


**Figure 20:** Residual Errors in the Validation Test for the 4<sup>th</sup> Order Discrete-Time State-Space Model (Left) and their Respective Autocorrelation

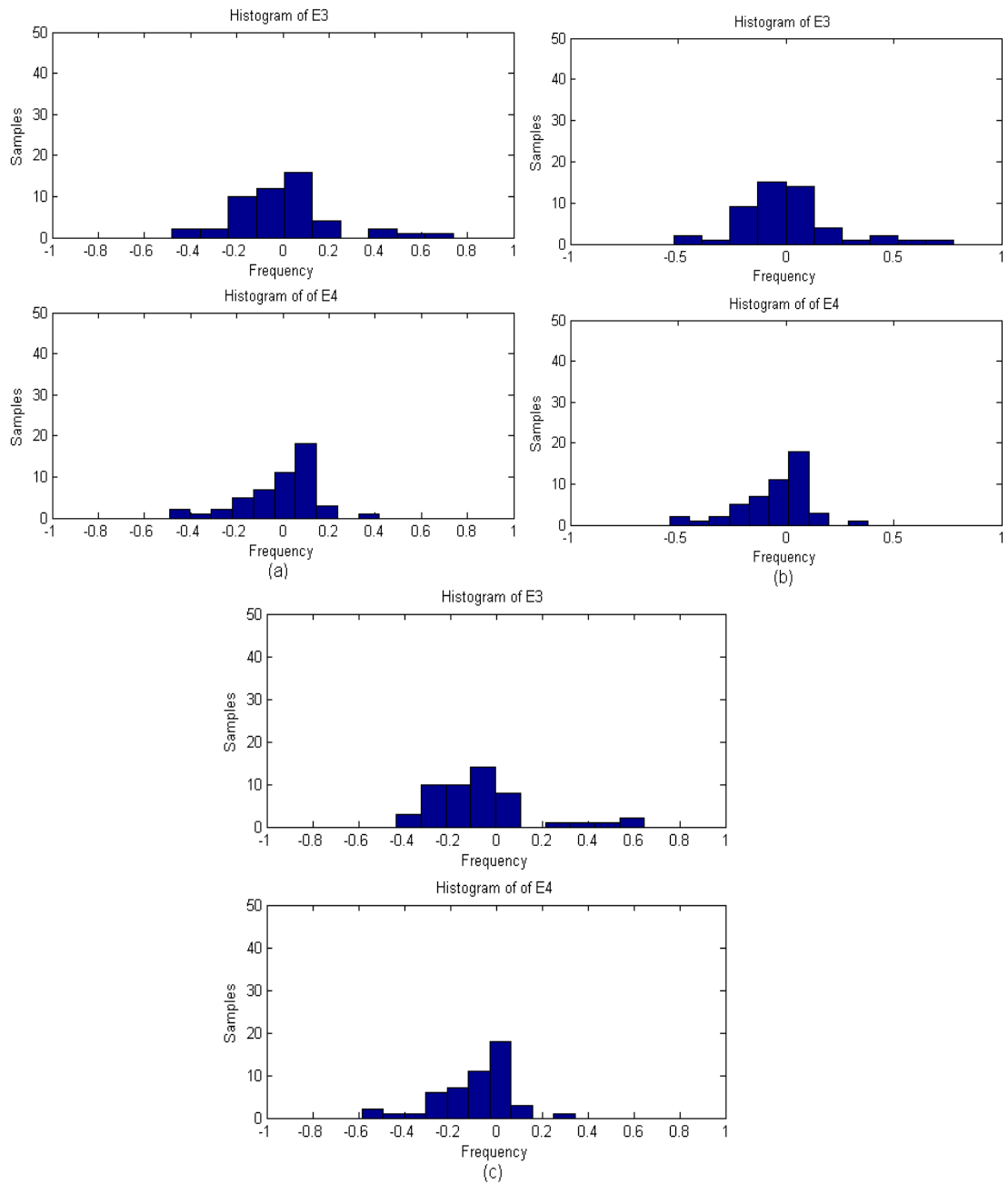


**Figure 21:** Histograms of the Residual Errors (a) 2<sup>nd</sup> Order Model, (b) 3<sup>rd</sup> Order Model, and (c) 4<sup>th</sup> Order Model

#### 4.4.2 Conditioned Space Modeling

The conditioned space described in Chapter 2 will be the plant to be controlled. The input variables for this system that influence its dynamical behavior are: (i) the mass flow rate of supply air to the conditioned space (that can be changed by changing the AHU fan speed) and (ii) the mass flow rate into the chilled water loop. Since we considered constant the flow rate of supply air to the conditioned space, the only input variable that can be varied is the mass flow rate into the chilled water loop ( $\dot{m}_{cw}(t)$ ). The output variable considered in this test is the temperature in the conference room ( $T_{conf}$ ).

It is very important to note that the relative humidity has no been considered in the conditioned space model. This parameter has a marked effect on the objective of maintaining comfort in the space to be cooled.

Despite the fact that many of the components comprising an HVAC system are most accurately modeled as nonlinear distributed parameter systems, low-order linear models are used to determined parameters for the local-loop controllers [33]. Many of the most commonly used process transfer function models for designing the local loop controllers can be represented by the following transfer function

$$G_p(s) = \frac{K e^{-sT_d}}{(s + p_1)(s + p_2)} \quad (19)$$

where  $\left(\frac{K}{p_1 p_2}\right)$  is the static gain,  $T_d$  is the time delay, and  $p_1$  and  $p_2$  are the reciprocals

of the time constants  $\tau_1$  and  $\tau_2$  of the system.

From the point of view of identification for control, estimation of a process given by Equation (19) is no different from estimating any other parameterized linear model.

The model in Equation (19) can be written as

$$G(s, \theta) \quad (20)$$

where  $\theta$  comprises the model parameters  $K, p_1, p_2,$  and  $T_d$ . To estimate these parameters, experimental data can be collected at a constant sampling interval  $T$ . If the model given by Equation (20) is sampled with this sampling interval, according to the input sampling interval (e.g. zero-order-hold) giving the discrete-time model

$$G(q, \theta) \quad (21)$$

where “ $q$ ” is the shift operator and works similar to “ $z$ ” in the Z-transform. A very natural approach to describe  $G$  in Equation (21) as a rational transfer function in the shift (delay) operator with unknown numerator and denominator polynomials is

$$G(q, \theta) = \frac{B(q)}{A(q)} = \frac{b_1 q^{-nk} + b_2 q^{-nk-1} + \dots \dots \dots b_{nb} q^{-nk-nb+1}}{1 + a_1 q^{-1} + \dots \dots \dots + a_{na} q^{-na}} \quad (22)$$

where there is a time delay of  $nk$  samples,  $nb$  coefficients in the numerator, and  $na$  coefficients in the denominator.

Fitting a process model to data, as described in Equation (19), is just a special case of prediction error identification, and can be implemented using the IDGREY model object in the Matlab<sup>®</sup> System Identification Toolbox. The experimental data to

estimate the conditioned space model was collected similar to the one collected for the absorption machine identification. Figure 22 presents the test performed for the identification of the conditioned space.

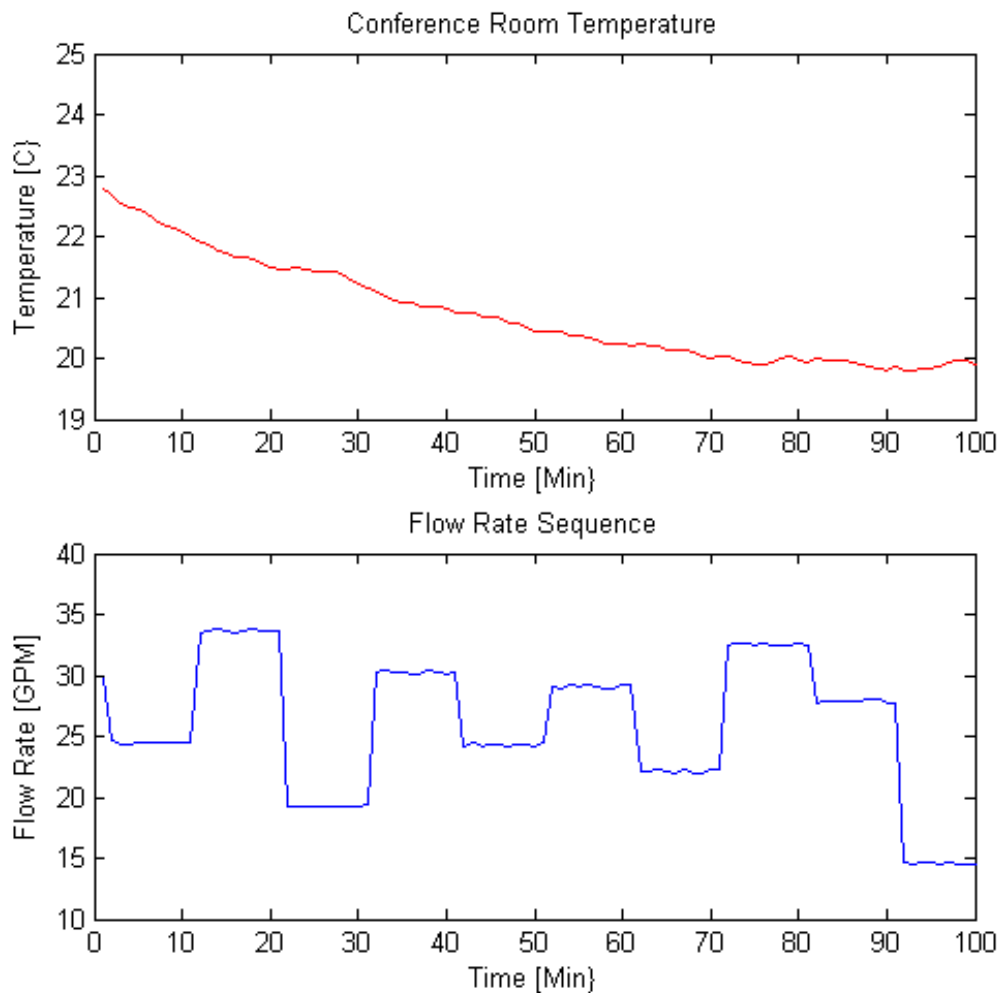


**Figure 22:** Experiment Data Set for Identification of the Conditioned Space. (a) Conference Room Temperature (b) Chilled Water Mass Flow Rate Sequence

The code program developed using Matlab<sup>®</sup>, basically uses two functions: (i) The first function is the function `IDDATA(Y,U,Ts)`. This function creates data object to

be used by identification routines.  $Y$  is the output data,  $U$  is the input data and  $T_s$  is the sampling time. (ii) The second function is the function on IDGREY ('Mfile Name', 'Parameter Vector', 'Cdmfile'). This function estimates a discrete-time model of the form of Equation(21). The 'Mfile Name' is the name of the file that describes the structure of the chosen model, the 'Parameter Vector' is the vector of nominal parameters, and the 'Cdmfile' determines if the estimated model is continuous or discrete. Both functions can be found in the System Identification Toolbox of Matlab<sup>®</sup>.

The IDGREY model object identified the following discrete-time transfer function

$$G(q, \theta) = \frac{0.0005823q^{-1} + 0.0005456}{q^{-2} - 1.82q^{-1} + 0.8223} \quad (23)$$

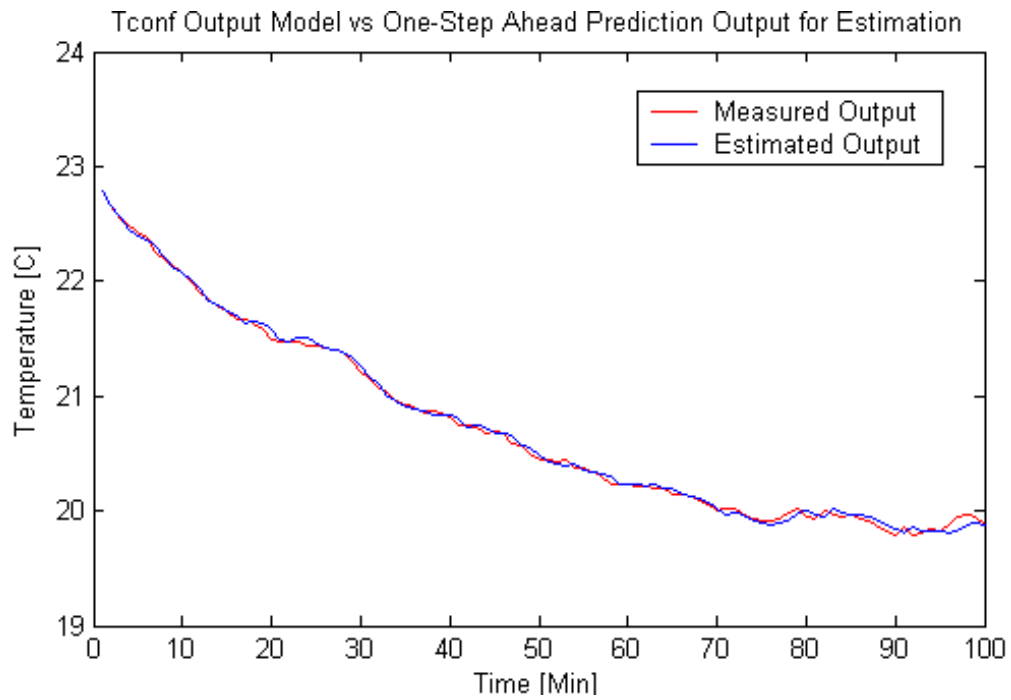
Using the D2C function from the Matlab<sup>®</sup> Control System Toolbox and the "zero order hold" intersample behavior, we have the continuous transfer function.

$$G(s) = \frac{3.45 * 10^{-7}}{(s + .00305)(s + 0.00021)} \quad (24)$$

A Matlab<sup>®</sup> code was developed to estimate the dead time. The resulting  $T_d$  was 41.3 seconds. The final rational transfer function of the form of Equation (19) was

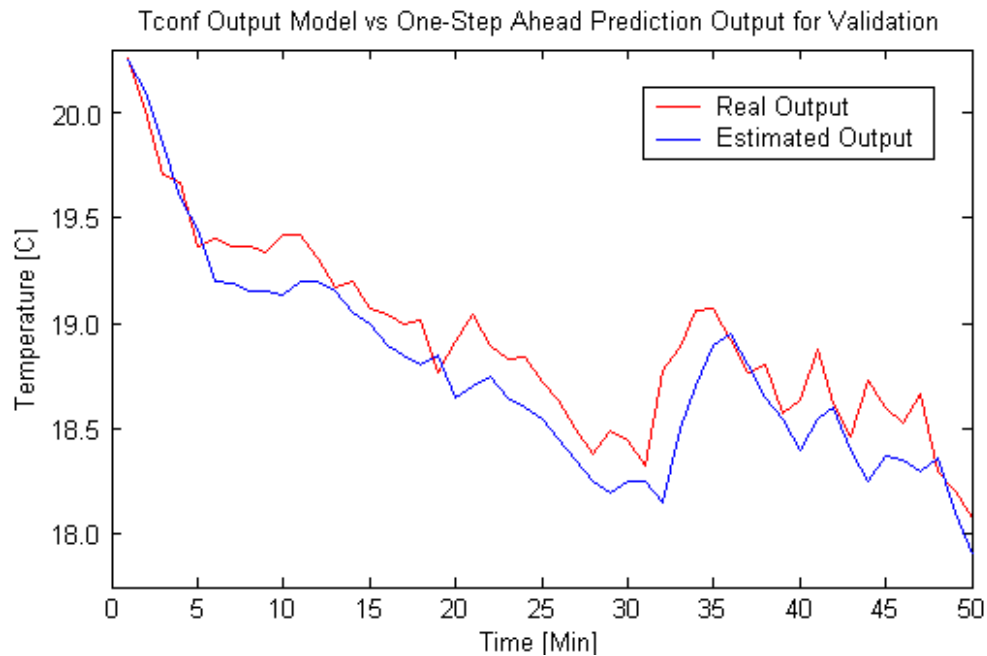
$$G(s) = \frac{3.45 * 10^{-7}}{(s + .00305)(s + 0.00021)} e^{-41.3s} \quad (25)$$

Figure 23 shows the model fit for the conditioned space. From this figure, it is seen clearly that the estimated model gives a reasonable description of the system.



**Figure 23:** Measured and Estimated Output Given by the IDGREY Function

The results of the validation are shown in Figures 24 and 25. Figure 24 shows the measured output and its estimated value for the validation test of the conference room.



**Figure 24:** Validation Test for the Identification of the Temperature in the Conference Room

Figure 25 shows the residual analysis for the validation test. The first plot shows the residual errors, the second plot shows the autocorrelation of the residual errors, and the third plot shows the respective histogram. From Figure 25, it is seen that the residual errors are not correlated and the error plotted in the histogram is only due to white noise. The length of the validation data was a set of 50 samples. From the resulting estimated model, we are able to design the temperature controller.

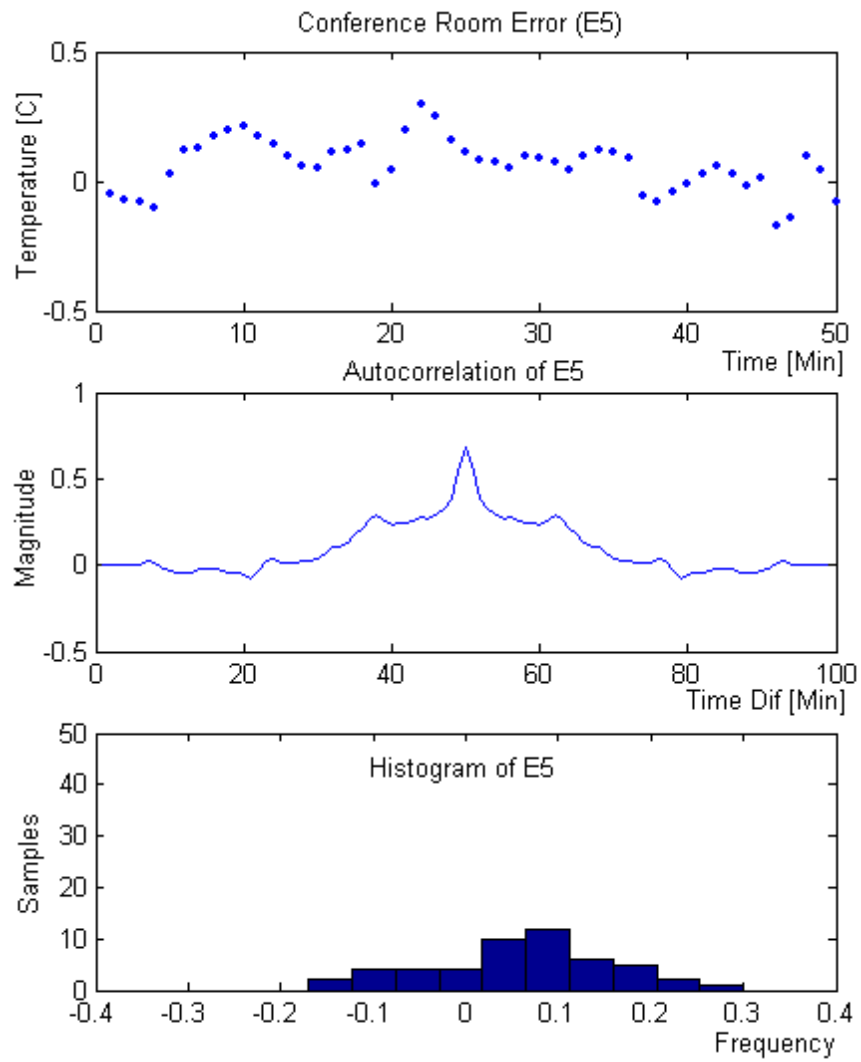


**Figure 25:** Residuals Analysis for the Validation Test (a) Residual Errors, (b) Autocorrelation of the Residual Errors, and (c) Histogram of the Residual Errors

## Chapter 5

### Controller Design and Implementation

This chapter presents the design and implementation of the temperature controller that regulates the temperature in the conditioned space. Developing such a controller and implementing it on the existing SAACS control and monitoring station required the analysis of two stages: The first stage was to design a classical Proportional-plus-Integral (PI) controller to control the estimated model of the plant described in the previous chapter. This design was evaluated with simulations generated Simulink<sup>®</sup> and the RLTOOL contained in Matlab<sup>®</sup>. The second stage was to develop a virtual instrument (VI) using the LabVIEW<sup>®</sup> software which was used to implement the designed controller. This control architecture was finally incorporated on the existing SAACS control and monitoring station developed by Meléndez. The analysis of the system's performance with the temperature controller is presented and discussed.

#### 5.1 Temperature Controller Design

Figure 26 shows the closed-loop control structure chosen for temperature control in the conditioned space. A proportional valve is used to regulate the flow in the chilled water loop. This valve is referred to as the actuator. When the user establishes a temperature set point, the controller receives an error signal (the difference between the set point and the actual system output) and computes the control signal to be sent to the

actuator. The actuator receives the control signal and regulates the flow rate is established. The plant receives this flow rate and after of a determined time the desired temperature is reached.

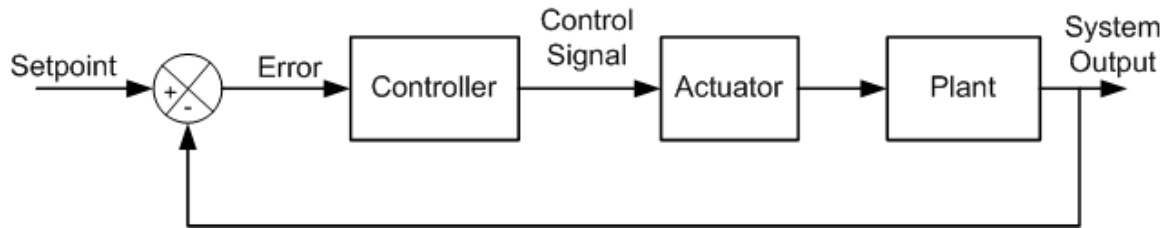


**Figure 26:** Closed-Loop Control Structure for the Temperature Control in the Conditioned Space

The temperature controller was designed to meet performance criteria of zero steady-state error with a little overshoot. The design tool used for this controller was the RLTOOL contained in Matlab<sup>®</sup>. This tool uses the Root-Locus method to assist on the design and performance evaluation of a single-input single-output (SISO) linear controller of any desired structure. To meet the design criteria, a Proportional-plus-Integral (PI) controller was selected. The integral action of the controller is required to add an integrator in the loop and guarantee zero steady-state error.

The estimated transfer function for the conditioned space was developed in the system modeling section and is reproduced here for convenience

$$G_p(s) = \frac{3.45 * 10^{-7}}{(s + .00305)(s + 0.00021)} * e^{-41.3s} \quad (26)$$

Using a 2<sup>nd</sup> order Padé approximation for the time delay results in the following rational transfer function

$$G_p(s) = \frac{3.45e - 007 s^2 - 5.012e - 008s + 2.427e - 009}{s^4 + 0.1485 s^3 + 0.00751s^2 + 2.303e - 005 s + 4.506e - 009} \quad (27)$$

This rational transfer function allows a design by the Root Locus method. Using the RLTOOL with the specified design criteria, the PI controller designed resulted in the following transfer function

$$G_c(s) = \frac{0.000442(s + 0.897)}{s} \quad (28)$$

This is a PI controller with a proportional gain  $K = 0.000442$  and integral time  $T_i = 1.115$  seconds. To simulate the controller's response, a step function was used. Simulations using Matlab<sup>®</sup> and Simulink<sup>®</sup> were developed. Figure 27 shows the results for the Matlab<sup>®</sup> simulation. From this figure, we can see that the control variable (mass flow in the chilled water loop) oscillates around of its operating point (that is approximately 26 GPM) to varied the control signal. With this control action we met the performance criteria of zero steady-state error and a setting time of 3860 seconds. Physically, this time is the period of time that the controller needs to remove the thermal capacity when the controller starts at the same time with the absorption machine.

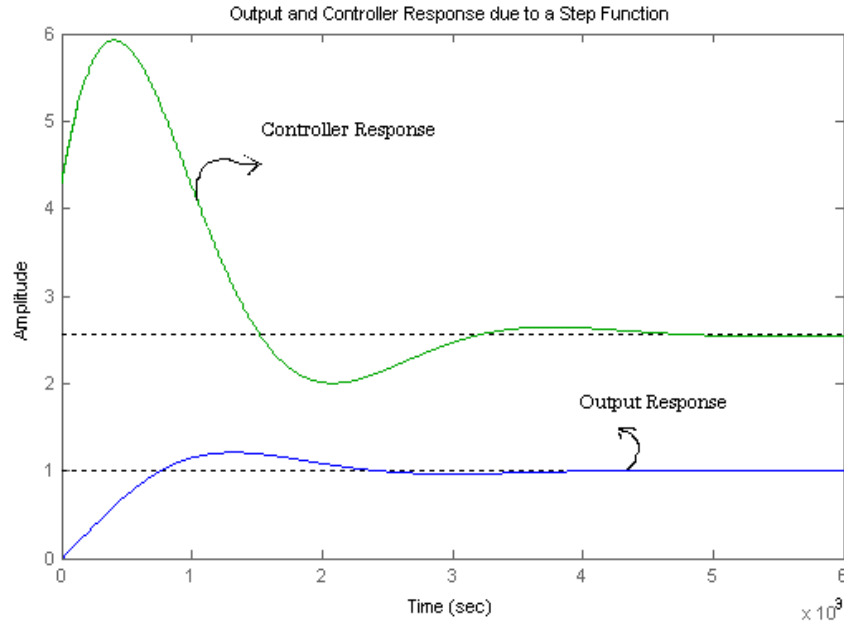


**Figure 27:** Closed-Loop Step Response and PI Controller Response for the Conditioned Space Simulated with Matlab<sup>®</sup>

A simulink block diagram is shown in Figure 28. The results of the simulation are shown in Figure 29 (a and b). The plots show the output response to the given set point (a desired temperature of 25 °C) and the error between the reference and the actual temperature of the conditioned space. Note that the input signal (set point) sends a command to reach a desire temperature. The response shows that the output follows the command without error and a little overshoot. The response also exhibits a long settling time (approximately 4000 seconds). The control action required to reduce this settling time would be greater than the designed controller can deliver because of the practical limitations in the flow rate range.

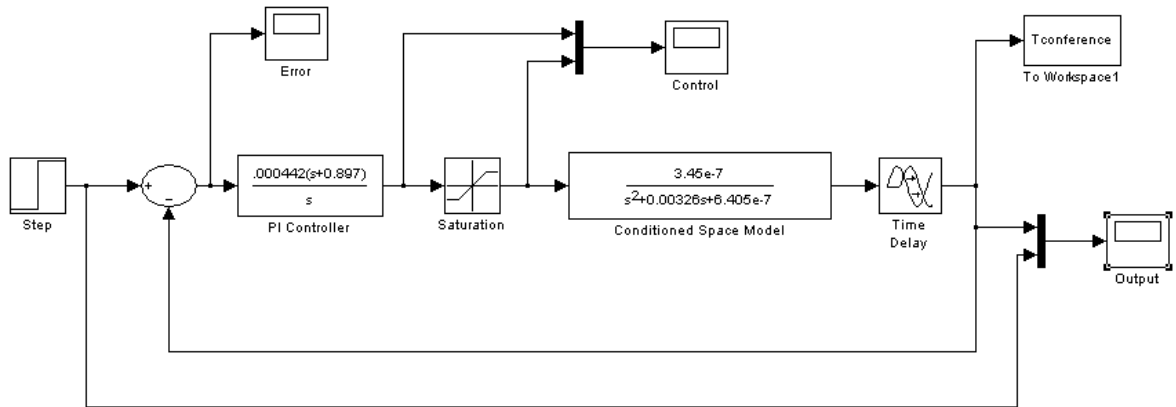


**Figure 28:** Simulink Block Diagram for the Temperature Control in the Conditioned Space

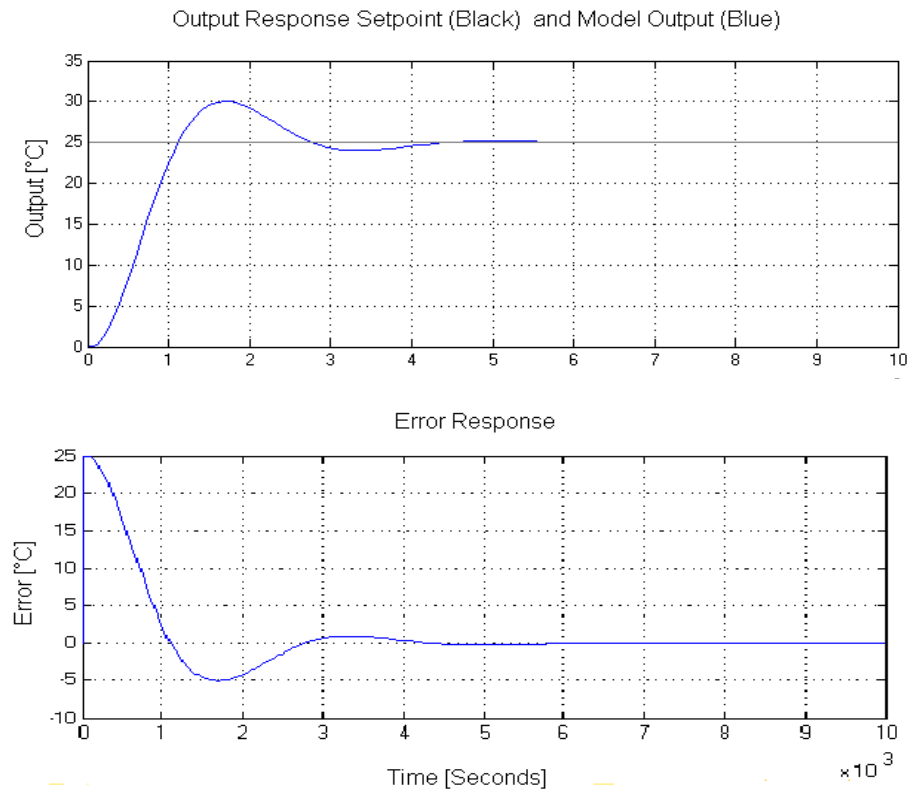


**Figure 29:** Simulink Results of the Temperature Controller for the Conditioned Space

## 5.2 Temperature Controller Implementation

The full implementation of the proposed temperature controller on the SAACS prototype at the Cabo Rojo site was achieved and is described in this section. The new controller was incorporated to the existing SAACS control and monitoring station developed by Meléndez [6]. Before describing the methodology of implementation of such controller, it is necessary to explain some aspects considered during the implementation.

Initially, the temperature controller was started when the absorption chiller started to operate. Due to the large error in temperature at startup, the control action will grow very large. This implementation was not possible. The reason is very simple, when the SAACS starts operation, the required control action can not be met by the controller, this means that the required flow to remove the thermal load in the conditioned space at startup would be greater than the controller can give. There are some limitations in the flow rate range in the chilled water loop (5-36 GPM).

To avoid the described problem, the control scheme in the chilled water transient response developed by Meléndez is used. The focus of this control scheme was to reduce the transient response of the chilled water line to enable faster operation of the absorption chiller in producing effective cool air. The control loop for this objective assumes that the operating conditions for the cooling tower and the generator heat input are met.

The strategy developed was as follows: when the absorption chiller starts to operate the flow sub-controller developed by Meléndez is used. This sub-controller regulates the flow rate in the chilled water line to reach the operating point, which is

around 8 and 10 °C. When this operating point is reached, both the air handling unit (AHU) and the temperature controller are started and connected to the control loop. In other words, the AHU and the temperature controller must wait for the chilled water line to reach its operating point before starting. Once the chilled water temperature has reached its operating point, the temperature controller must compensate the temperature of the conditioned space requested by the user. The actual temperature of the conditioned space is thus used to feedback the controller. When the controller determines a difference between the desired temperature and the actual temperature, it will regulate the chilled water flow to reach the desired temperature. Figure 30 shows the block diagram for the strategy to incorporate the proposed temperature controller to the SAACS prototype

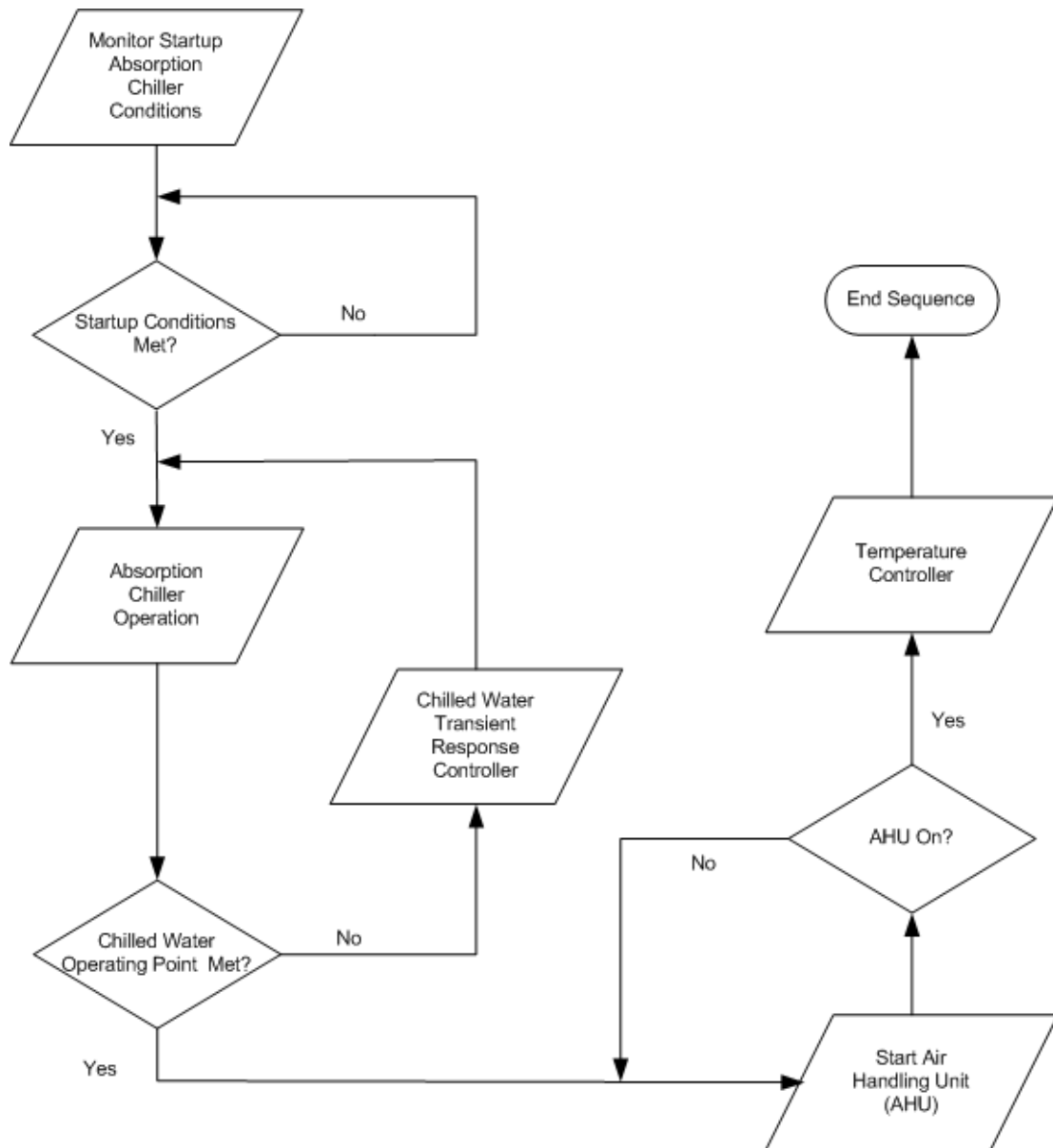


**Figure 30:** Block Diagram to Incorporate the Temperature Controller to the SAACS Prototype

The implementation of the previously control decision on the SAACS prototype was performed by a control subroutine in LabVIEW<sup>®</sup>. This subroutine was then incorporated on the one developed by Meléndez [6]. Figure 31 shows the subroutine developed by Meléndez while Figure 32 shows the new subroutine incorporating the proposed temperature controller to control the two proportional valves in the SAACS system. The main difference between these two subroutines is the feedback signal to control the proportional valve. The temperature controller regulates the flow rate in the chilled water line based on the measurement of the actual temperature of the conditioned space. The temperature controller starts to operate simultaneously with the AHU. The controller for the proportional valve developed by Meléndez takes the flow rate as feedback signal and only works during the transient response in the chilled water line.

In Figures 31 and 32 each PID block, the derivative time  $T_d$  is set to a value of zero, thus making the blocks act as PI controllers. The gains for the PID boxes can be changed on line in the front panel of the subroutines that can be accessed from the SAACS control and monitoring station. Also, after each PID block, there is a saturation block that does not allow the output of the controller to be lower than 0 or higher than 1. This restriction block is applied to the controller's output, the control signal is scaled for the minimum and maximum allowed voltages for the chilled water proportional valve

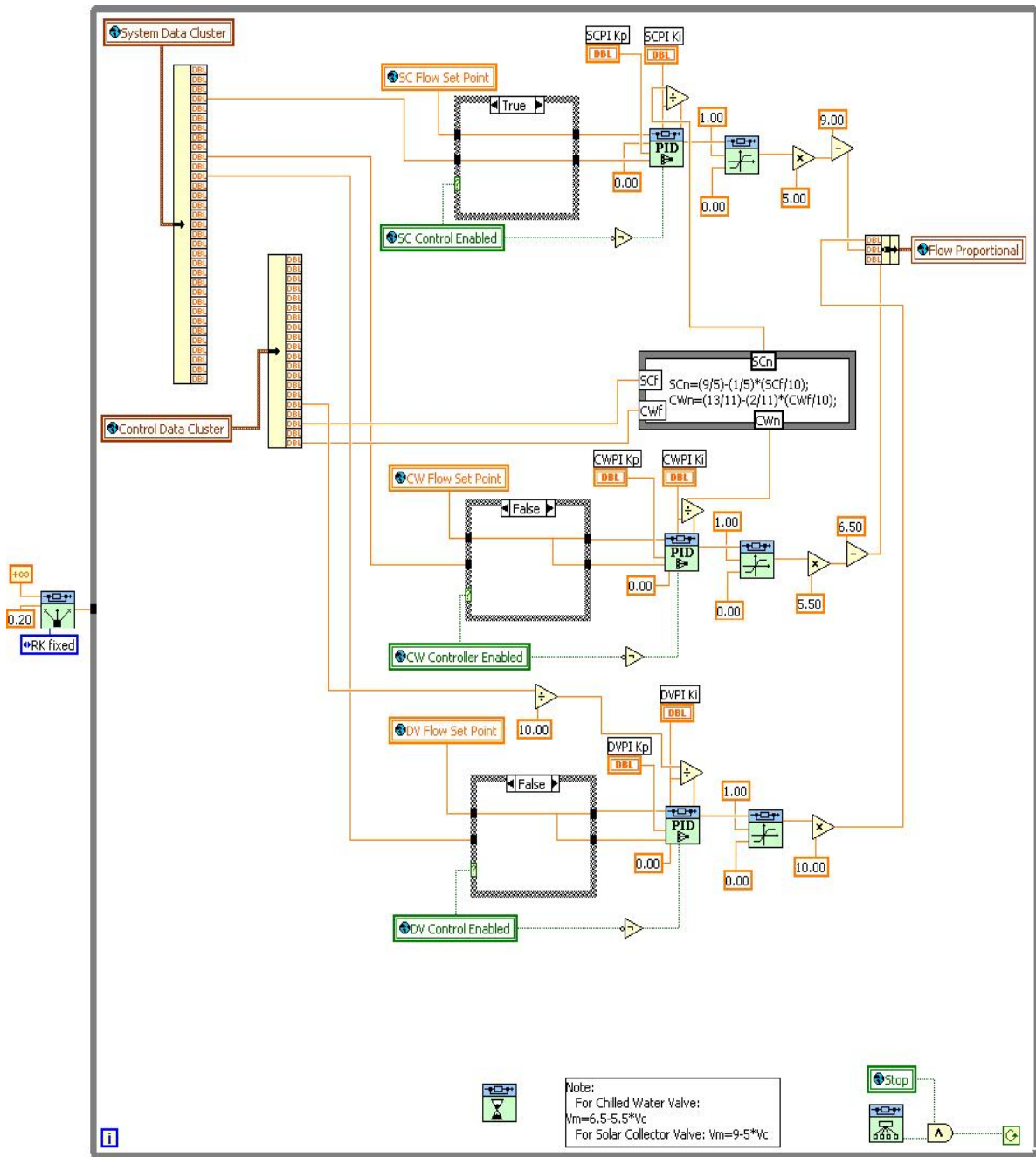
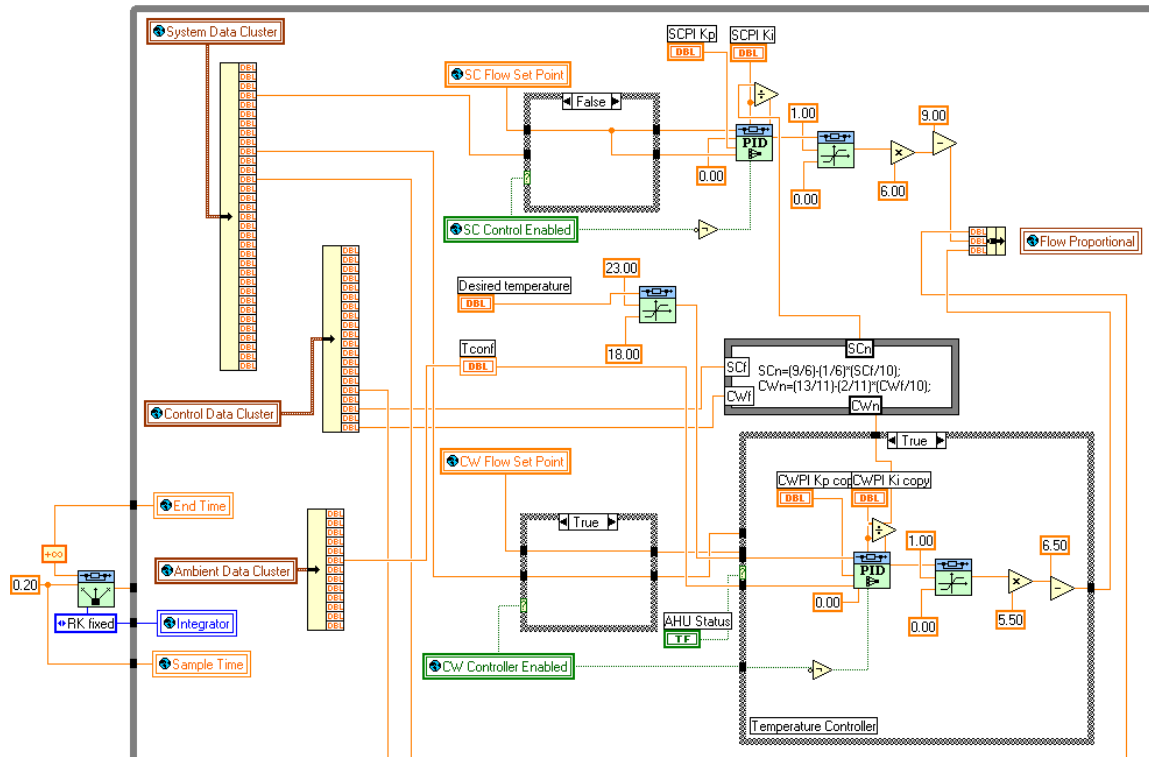


Figure 31: Block Diagram for the Flow Rate Controller Developed by Meléndez [6]



**Figure 32:** Modified LabVIEW Subroutine to Implement the Proposed Temperature Controller

The SAACS Graphical Visualization Window [6] was used to display the temperature response for the conditioned space when the controller's output signal to the proportional valve is set based on the temperature set point requested by the user. Figures 33 and 34 show the implementation results. From figure 33 we can see that command signal establishes a desired temperature value of 25°C, at this point the temperature control started to work. Then, the set point value is changed to 22.3°C as soon as the controller is enabled. The set point is again changed to a value of 19.4 °C and finally set to 23.3°C. Figure 34 shows the control action during this test. The control

signal is varied according to the required flow rate in the chilled water line to reach the each temperature set point established in Figure 33.

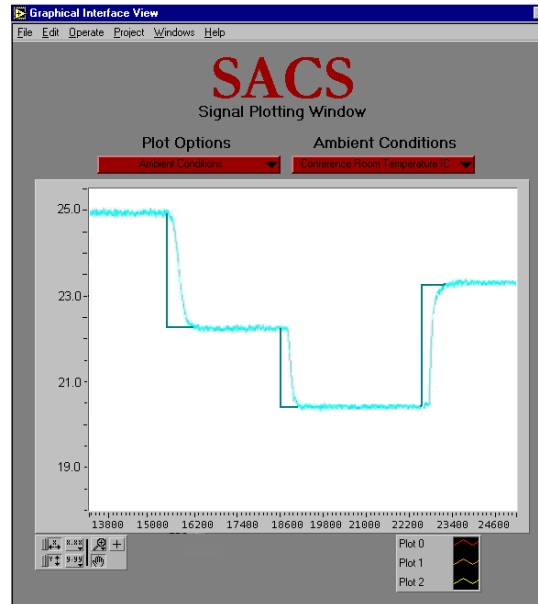


**Figure 33:** Actual temperature vs. Desired Temperature Setpoint in the Conference Room

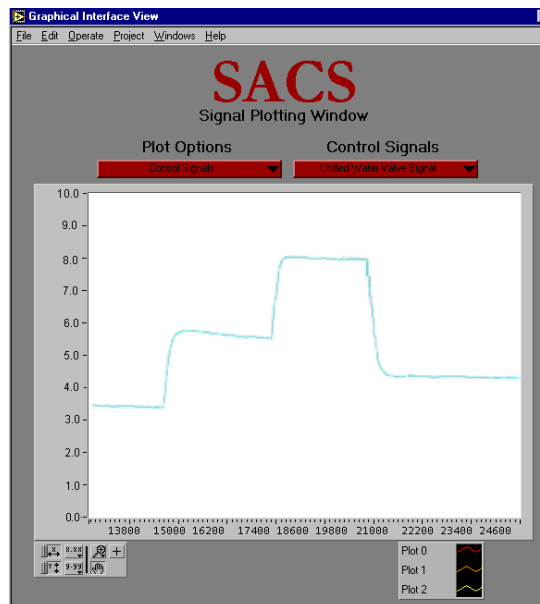


**Figure 34:** Control Signal to Reach the Desired Setpoint

### 5.3 SAACS System's Performance Analysis

The main objective of this research was to design and implement a temperature controller on the SAACS prototype. This temperature controller will operate the absorption chiller under multiple load conditions. After implementing the proposed controller, an analysis of the system's performance is presented in this section.

To analyze the SAACS system's performance under the implemented the designed temperature controller, some variables of the SAACS control and monitoring station were monitored and plotted. The tests were performed under similar ambient conditions during the months of February and March of 2004 for available energy in the collectors and outdoor temperature to ensure a fair comparison of the results. These tests were also performed under similar conditions in the thermal stratified tank since the main objective of regulating the flow in the chilled water loop is to analyze the percent of energy consumption of the available energy in the thermal storage. If this percent can be reduced, we could extend the SAACS period of operation. Figures 35 and 36 shows the average outdoor temperature profile and the average outdoor humidity profile during the days that the tests were performed.

### Average Outdoor Temperature Profile

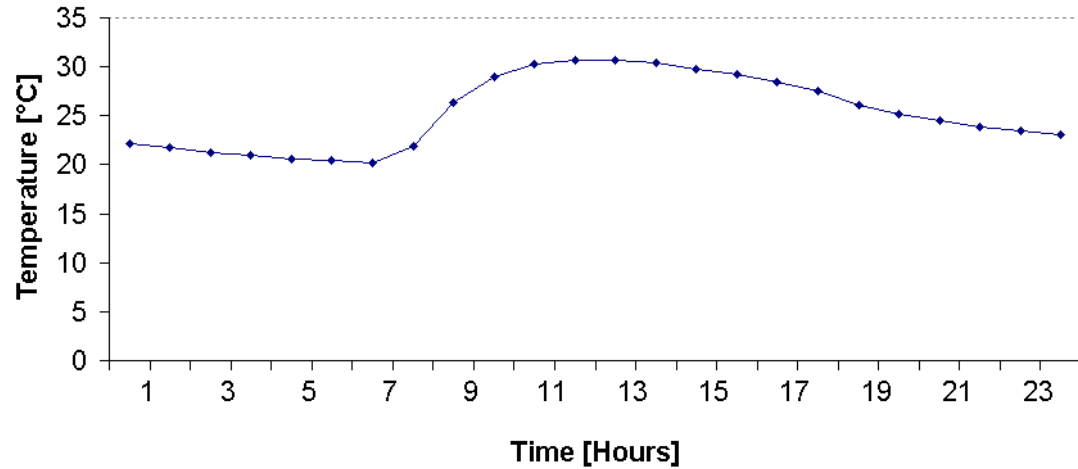


Figure 35: Average Outdoor Temperature Profile Used for the SAACS Performance Test

### Average Conditioned Space Humidity Profile

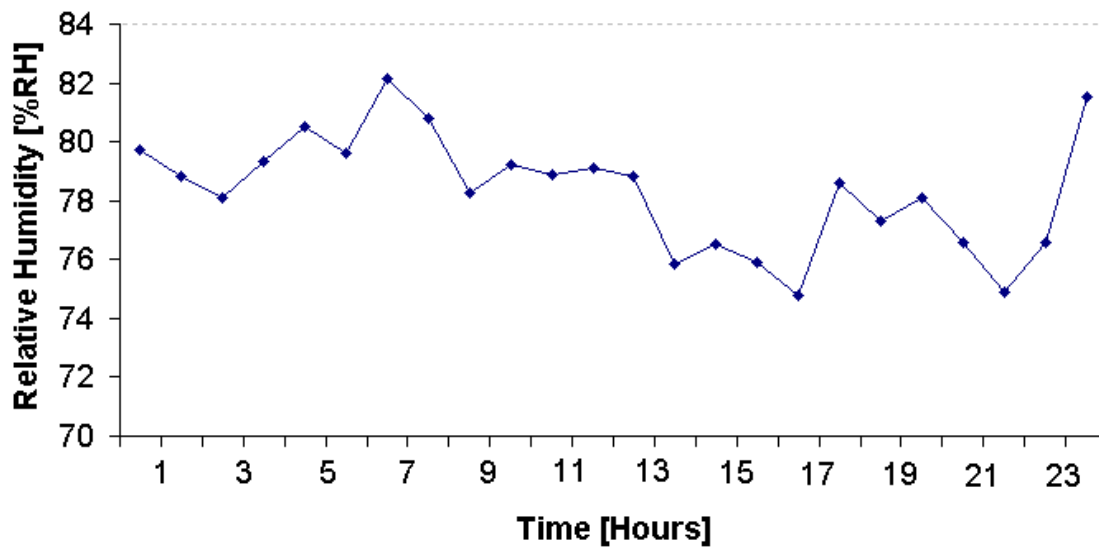


Figure 36: Average Conditioned Space Humidity Profile Used for the SAACS Performance Test

Implementing the temperature controller in the chilled water loop has considerably improved the performance of the thermal stratified tank. Figures 37 and 38 show the tank temperature profiles without the temperature controller and with the temperature controller respectively. From these figures we can observe that after implementing the temperature controller, the tank temperature profile decays slower than without the temperature controller. In others words, when the flow rate in the chilled water line is varied, the absorption chiller heat consumption can be reduced or increased accordingly. If the flow rate in the chilled water line is reduced, the absorption chiller heat input in the heat medium loop will be reduced. If the temperatures profile decrease slower, the absorption chiller will extend its period of operation to supply the cooling required by the thermal load (the conditioned space).

The test performed without the temperature controller was developed setting the nominal in the chilled water line (26GPM). For the test performed with the temperature controller, a “set point” of 23 °C was established.

Looking at the Figures 36 and 37 it is seen that when the SAACS operated under the temperature controller an extension in the period of operation was achieved (approximately 20 minutes).

### Tank Temperature Profile without Temperature Controller

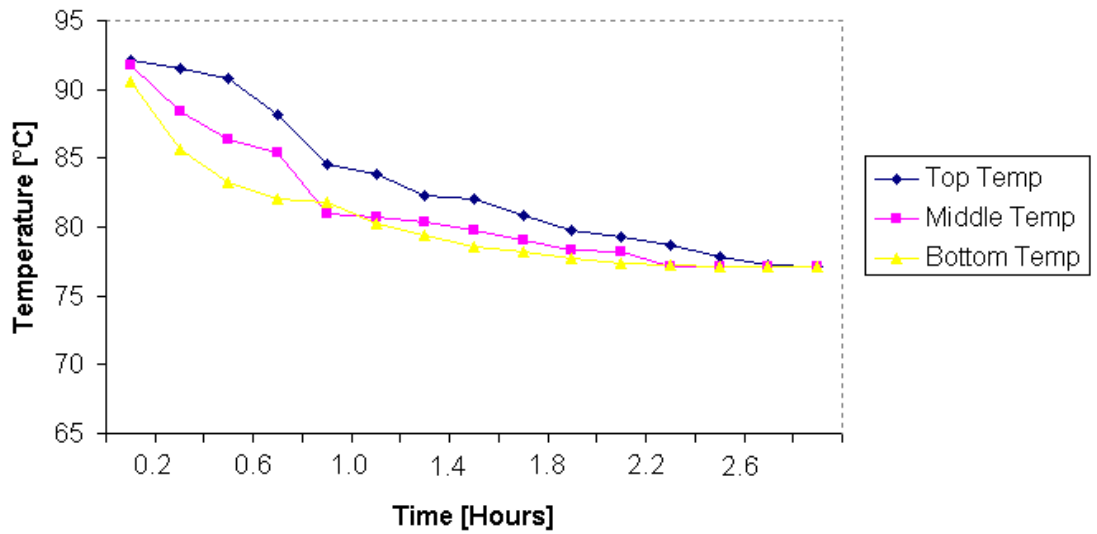


Figure 37: Thermal Stratified Tank Temperature Profile without the Temperature Controller

### Tank Temperature Profile with Temperature Controller

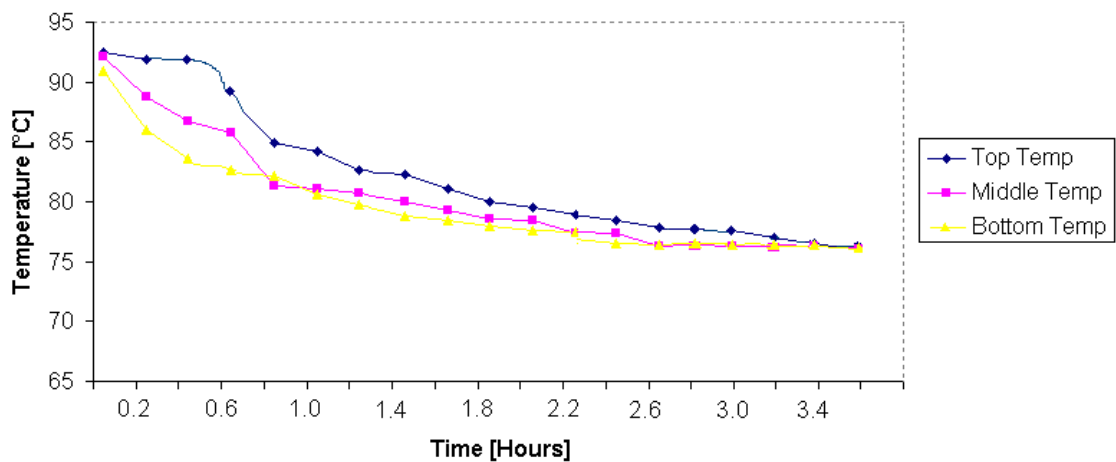
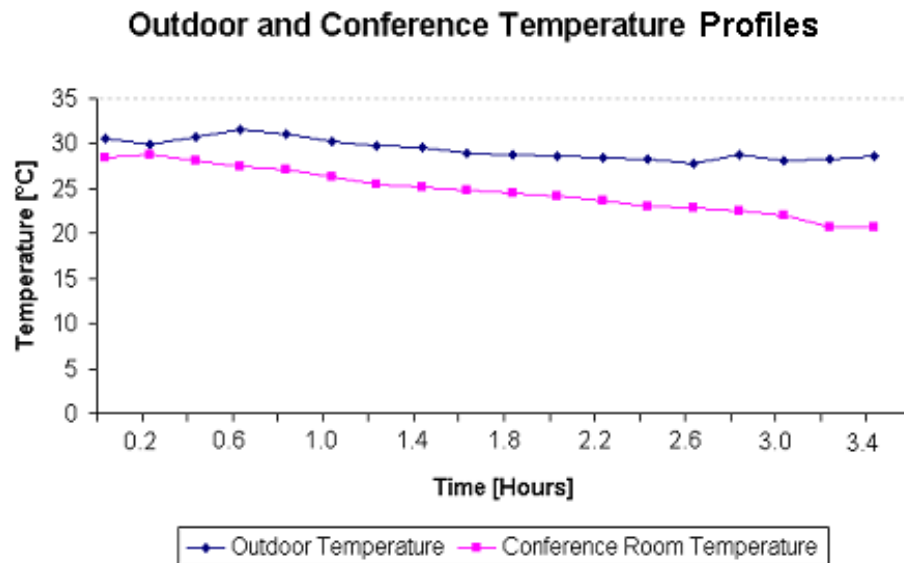


Figure 38: Thermal Stratified Tank Temperature Profile with the Temperature Controller

As explained before, the AHU was disabled until the chilled water line reaches its operating point. Melendez [6] established that if the chilled water line is operating as its nominal flow (approximately 26 GPM), the operating point is reached around 50-60 minutes. When the AHU is enabled, the temperature controller will regulate the flow rate to reach a desired temperature in the conditioned space.

Limitations in the chilled water flow range due to the capacity of the chilled water pump [approximately 5 – 36 GPM] and limitations in the improper position of the return air duct of the AHU are reflected in the temperature range in the conditioned space. The designed temperature controller only can cool the conference room temperature to 21 °C approximately. Figure 39 shows a comparison between the outdoor temperature and the conference room temperature during test performed with the temperature controller.



**Figure 39:** Comparison of Outdoor Temperature and the Conference Room Temperature Controlling the Temperature

To evaluate the system performance of the SAACS under the temperature controller, the coefficient of performance (COP), the average cooling load, and the overall SAACS efficiency were observed.

Figure 40 shows the COP for the test performed. The COP was determined by Meza as the ratio of generated cooling capacity to the input heat [5]:

$$COP = \frac{Q_{evaporator}}{Q_{generator}} \quad (29)$$

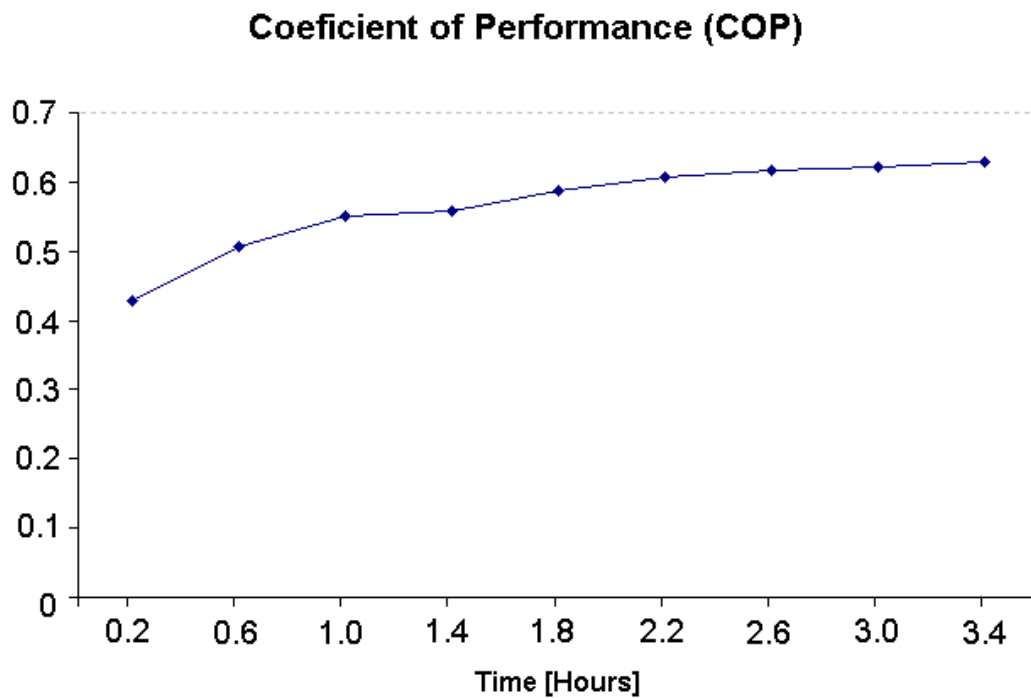


**Figure 40:** Coefficient of Performance (COP) for the Test Performed using the Temperature Controller

From Figure 40, it is seen that the COP achieved with the temperature controller is similar in comparison to the COP before implementing the temperature controller and described by Meléndez [6].

The last two performance criteria that provide insight of the performance of the SAACS prototype are the cooling load (heat produced in the evaporator) and the system overall efficiency. The cooling load was determined by Meza as [5]

$$Q_{evaporator} = .063 * \dot{m}_{cw} * 4200 * (T_{cwt_o} - T_{cwt_i}) \quad (30)$$

where,  $\dot{m}_{cw}$  is the flow in the chilled water line.  $T_{cwt_o}$  and  $T_{cwt_i}$  are the outlet and inlet temperatures in the chilled water line respectively. Figure 40 shows the cooling load during the test performed.

The overall efficiency of the system defined by Meza [5] as the amount of cooling that is generated with regard to the amount of solar energy being collected, is given by

$$\eta_{overall} = COP * \frac{Q_{evaporator}}{A_c * I} \quad (31)$$

where  $A_c$  is the collector array selective surface area and  $I$  is the solar radiation.

Figures 41 and 42 show the Cooling load and the overall SAACS efficiency respectively. From these plots, it is seen that both the cooling load and SAACS overall efficiency obtained with the temperature controller are similar to the ones obtained by

Meléndez. The main difference is that when the temperature controller operates, an extension of the SAACS period of operation can be achieved

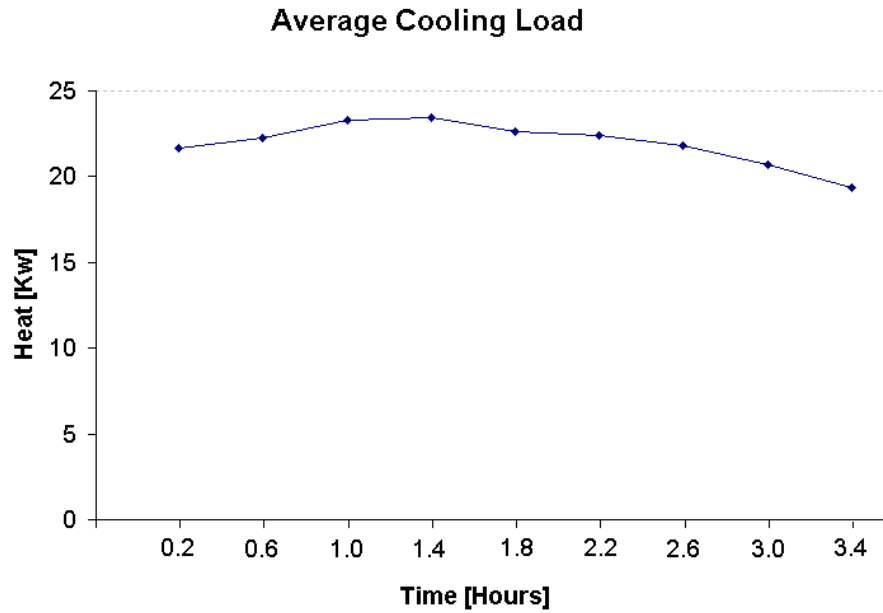


**Figure 41:** Average Cooling Load from the Absorption Machine

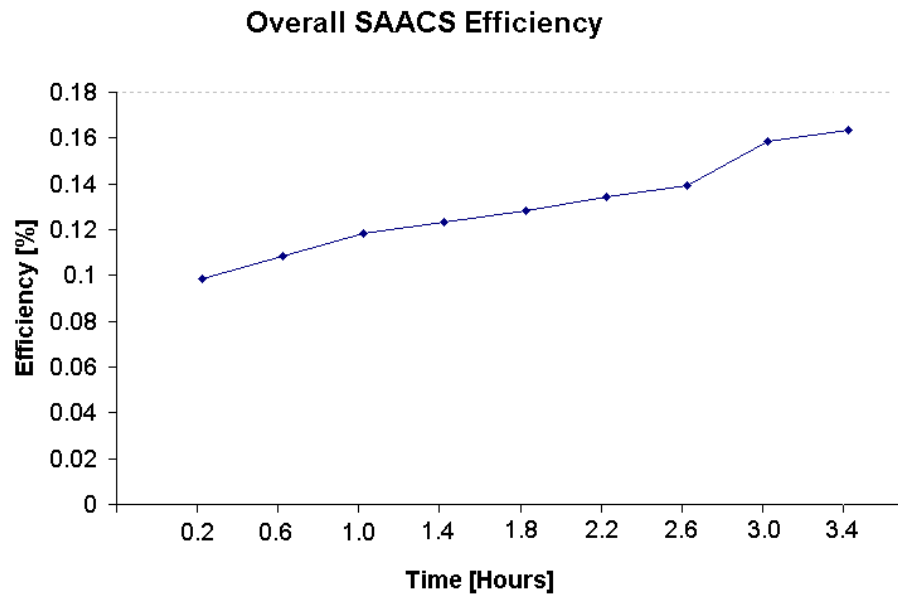


**Figure 42:** Overall SAACS Efficiency under the Temperature Controller

## Chapter 6

### Conclusions and Recommendations

The design and implementation of a temperature controller for the SAACS prototype has been achieved in this work. This temperature controller has considerably improved the performance of the SAACS prototype residing in Cabo Rojo, Puerto Rico.

For the absorption machine subsystem in the SAACS prototype, the use of variable flow rates in the chilled water line is reflected in the amount of energy available in the thermal storage. Reducing the flow in the chilled water line makes it possible to extend the period of operation of the SAACS while maintaining the comfort in the conditioned space. It was shown that the mass flow rate in the chilled water line affects the thermal storage temperature profile.

A “Black Box” model has been identified for the absorption machine. A second order state-space model has been estimated using the Matlab<sup>®</sup> Identification System Toolbox. This estimated model could be used for simulation and prediction purposes. With this model we do not have to deal with the classical complex dynamic models developed in previous works.

The results of this research contributed to extend the period of operation of the SAACS. The temperature controller allows the chiller to work under different load condition and proposes the same scheme that utilizes a commercial HVAC system unit (PI controller). An extension of approximately 20 minutes was achieved when the temperature controller was implemented.

The designed temperature controller could be implemented on the SAACS prototype located at Hato Rey, Puerto Rico. In this particular area, there are better ambient conditions and the capacity of the thermal storage is bigger. With this implementation, we will be able to explore the possibility of extending the operation hours of the system while controlling the conditioned space temperature.

For commercialization purposes, an important addition will be to incorporate the temperature control strategy on the actual microcontroller based platform control unit

An important area for further research would be the application of recursive system identification for the conditioned space. With this model, an adaptive temperature controller can be developed.

Another area for further research would be the design of a control system that achieves independent control over the temperature and relative humidity in the conditioned space. The relative humidity can have a marked effect on the control objective of maintaining comfort in the space to be cooled.

## References

- [1] Clifford, G., *“Modern Heating, Ventilating and Air Conditioning,”* New Jersey: Prentice Hall, 1990
- [2] *“Energy Conservation”* Online British Encyclopedic, May-2003
- [3] Bong, T. Y., Ng, K. C., and Tay, A. O., *“Performance Study of a Solar-Powered Air Conditioning System,”* Solar Energy, Vol.39, No. 3, pp. 173-182, 1987
- [4] Van Hattem, D., and Dato, P. A., *“Description and Performance of an Active Solar Cooling System, Using a LiBr-H<sub>2</sub>O Absorption Machine,”* Energy and Buildings, Vol. 3, pp. 169-196, 1981
- [5] Meza, J. I., Khan, A. Y., and González, J. E., *“Experimental Assessment of a Solar Assisted Air Conditioning System for Applications in Puerto Rico,”* Solar Engineering, pp. 149-154, 1998
- [6] Meléndez, L.V., *“Automation and Control of Solar Air Conditioning Systems,”* Master Thesis, University of Puerto Rico- Mayagüez Campus, 2000
- [7] Farber, E.A., Flannigan, F.M., Lopez, L., and Polifka, R.W., *“Operation and Performance of the University of Florida Solar Air-Conditioning System,”* Solar Energy, Vol. 10, pp 91-98, 1966
- [8] Bergquam, J.E., *“Solar Absorption Air Conditioning/Sacramento Municipal Utility District,”* Final Report to NREL under subcontract No. AR-2-12138-1, Bergquam Energy, Sacramento, California, 1993
- [9] Sayigh, A.A.M., and J.C. Mc Veigh, *“Solar Air conditioning and Refrigeration,”* Renewable Energy Series, Pergamos Press, 1992
- [10] Herold, K. E., Radermacher, R., and Klein, S. A., *“Absorption Chillers and Heat Pumps,”* CRC Press, Boca Raton, FL, 1996

- [11] Van Hattem, D., and Dato, P. A., "*Description and Performance of an Active Solar Cooling System, Using a LiBr-H<sub>2</sub>O Absorption Machine,*" Energy and Buildings, Vol. 3, pp. 169-196, 1981
- [12] Anand, D. K., Allen, R. W., and Kumar, B., "*Transient Simulation of Absorption Machines,*" Journal of Solar Energy Engineering, Transactions of the ASME 104, pp.197-203, 1982
- [13] Jeong, S., Kang, B. H., Lee, C. S., and Karng, S. W., "*Computer Simulation on Dynamic Behavior of a Hot Water Driven Absorption Chiller,*" Proceedings of the International Absorption Heat Pump Conference 31, American Society of Mechanical Engineers, Advanced Energy Systems Division, pp. 333-338, 1994
- [14] Zhuo, C., "*Absortion Heat Transformer with TEF-Pyr as the working Pair,*" Ph. D. Thesis, Delf University of Technology- Netherlands, 1995
- [15] Stephan, K., and Schmitt, M., "*Dynamics of a Heat Transformer Working with Mixture NaOH-H<sub>2</sub>O,*" Int. Journal of Refrigeration, Vol. 7, pp. 483-495, 1997
- [16] Hernández, H., "*Analysis and Modeling of a Solar-Assisted Air Conditioning and Dehumidification System for Application sin Puerto Rico ,*" Master Thesis, University of Puerto Rico- Mayagüez Campus, 1997
- [17] Hammad, M., Zurigat, Y., "*Performance of a Second Generation Solar Cooling Unit,*" Solar Energy, Vol. 62, No. 2, pp. 79-84, 1998
- [18] Chow, T. T., Lin, Z., and Song C. L., "*Applying Neural Network and Genetic Algorithm in Absorption Chiller Modeling,*" Seventh International IBPSA Conference, pp. 1059-1066, 2001
- [19] Alva, L.H., "*Air-Cooled Absorption Machine with Solar PCM-Collectors for Applications in Tropical Climates ,*" Master Thesis, University of Puerto Rico- Mayagüez Campus, 2002

- [20] Fu, D., Lu, Z., Cao, W., and Zhang, W., "*Dynamic Simualtion of a Gas-Fired Double-Effect Lithium Bromide Absorption Chiller,*" Proc. Int. sorption Heat Pump Conf., pp. 189-193, 2002
- [21] Kim, D. S., Wang, L., and Machielsen H. M., "*Dynamic Modeling of a Small-Scale NH<sub>3</sub>/H<sub>2</sub>O Absorption Chiller,*" Int. Congress of Refrigeration, Vol.2, pp. 210-217, 2003
- [22] Anderson, S. A., and Dieckert, J., "*On-Site Chiller Testing,*" ASHRAE Journal Vol. 32, pp. 54-60, April-1990
- [23] Aoyama, M., and Izushi, M., "*Chilled Water Response of a Gas-Fired Single-Effect Lithium Bromide Absorption Chiller due to Disturbances in the Heat Source,*" Hitachi Review, Vol. 39, No 3, pp. 149-154, 1994
- [24] Haves, P., Salsbury, T., and Wright, J., "*Process Fault Detection Methods of a Gas-Fired Absorption Chiller via Parameter Estimation,*" ASHRAE Transactions, Vol. 102 pt. 1, pp. 519-527, 1996
- [25] Priya, S., "*Comparison of Chiller Models for use in Model-Based Fault Detection,*" Master Proyect (Plan II), University California- Berkeley, 2001
- [26] Argüello Serrano, B.C., "*Nonlinear Controller For An HVAC System With Thermal Load Estimation,*" Master Thesis, University of Puerto Rico at Mayagüez, 1994.
- [27] Federspiel, C. C., Asada, H., "*Adaptive Control of Thermal Comfort Based on Human Thermal Sensation,*" Dynamic Systems and Control Series, ASME, Vol. 33, pp. 161-168, 1991
- [28] Rentel, C.H., "*Nonlinear Decoupling of Temperature and Relative Humidity for an Air Conditionign System,*" Master Thesis, University of Puerto Rico- Mayagüez Campus, 1996

- [29] Ljung L., "*Identification for control: Simple Process Models*," Proceedings of the 41<sup>st</sup> IEEE Conference on Decision and Control. Las Vegas, Nevada USA, pp. 4652-4657, 2002
- [30] Van Den Hof, P.M., and Schrama, R.J., "*Identification and Control-Close Loop Issues*," *Automatica*, Vol. 31, pp. 1751-1770, 1995
- [31] Kosut, R.L., Goodwin, G.C., and Polis, M.P., "*Especial Issue on System Identification for robust Control Design*," *IEEE Trans.*, Vol. 37, 1992
- [32] Zang, Z., Bitmead, R.R., and Gerves, M., "*Iterative Weighted Least Squares Identification and Weighted LQG Control Design*," *Automatica*, Vol. 31 (11), pp. 1577-1594, 1995
- [33] Federspiel, C. C., and Seem, J. E., "*Temperature Control in Large Buildings*," Chapter 70, *CRC Control Handbook*, Ed. W. S. Levine, CRC Press. 1996
- [34] American Yazaki Corporation, "Installation & Service Manual for Water Fired Chillers". 1996
- [35] Ljung L., "*System Identification-Theory for the User*," PTR. Prentice Hall, New Jersey 1987
- [36] Haves, P. "*Overview of Diagnostics Methods*," Proceedings of Diagnostics for Commercial Buildings: From Research to Practice, San Francisco, CA. 1999. <http://poet.lbl.gov/diagworkshop/proceedings/haves.htm>
- [37] P. Van Overschee and B. De Moor, "*N4SID: Subspace algorithms for the identification of combined deterministic-stochastic systems*," *Automatica*, Vol. 30, No 1, pp. 75-93, 1994
- [38] Ljung, L., "*Estimation focus in System Identification: Prefiltering, Noise Models, and Prediction*," Proceedings of the 38<sup>th</sup> Conference on Decision and Control, Phoenix, Arizona, USA, 2810-2815, 1999